

2.4 Local measures

2.4.1 Local shelter of residential areas

From Chapter 2.2 we learned that the impact of relatively small linear open spaces as railways and highways perpendicular on wind is substantial. Wind sheltering action has to be taken as close to the residential area as possible. That is why we shift our attention some kilometres into a cutout with its zero point in Rokkeveen itself (8 'hour' South West see Fig. 252). This residential area is not separated from its foreland by a highway or wide water. So, shelter can adjoin immediately to residential area.

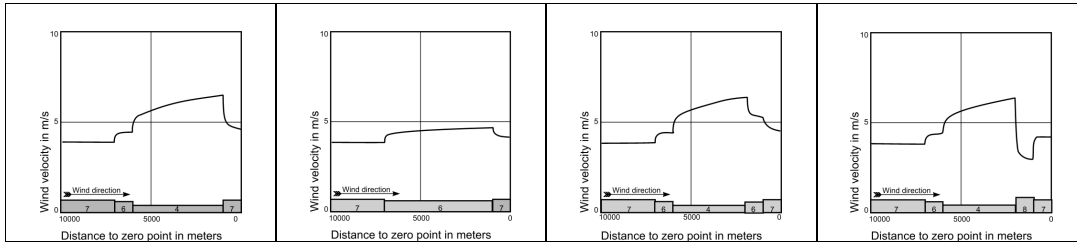


Fig. 271 Reference windvelocity

Fig. 272 Delt -> Rokkeveen with 6km green structure

Fig. 273 Delt -> Rokkeveen with 1km regular forest

Fig. 274 Delt -> Rokkeveen with 1km heavy forest

In Fig. 271 we suppose above Delft a stable velocity of less than 4 m/sec. Above 1km Delftse Hout it climbs up and stabilises on 4.5 m/sec in a few hundred metres. Then above 5 km farmland it starts to climb up fast continuing to increase more slowly to 6.52 m/sec. Then above Rokkeveen it slows down fast to 4.61 m/sec and outside the graph slowly to 4.2 m/sec above above suburban built up area. In Fig. 272 farmland is replaced by green structure (roughness 6). Then wind velocity at the edge of Rokkeveen decreases substantially from 6.52 to 4.73 m/sec. Energy loss per non airtight dwelling per year as far as due to wind from this direction decreases 190 kWh only (from 987 kWh to 797 kWh). If the last km before Rokkeveen would have been replaced by green structure only, velocity would reduce to 5.23 m/sec. Ventilation loss would still reduce by 141 kWh. Would 1km roughness higher than 6 have more impact?

In Fig. 273 and Fig. 274 only the last km before Rokkeveen farmland (roughness 4) is replaced by regular forest (roughness 7) and heavy forest (roughness 8). From these thought experiments we conclude 1km regular forest has approximately the same impact as 6km green structure. However, 1km heavy forest with rather high trees (15m) reduces wind velocity substantially to 2.90 m/sec at the edge of town. Energy loss per non airtight dwelling per year as far as due to wind from this direction there decreases 324 kWh from 987 kWh to 663 kWh. However, above suburban built up area wind velocity increases again fastly stabilising on approximately 4.2 m/sec.

Fig. 275 and Fig. 276 compare regional remote (see 2.3.5) and locally adjacent (see above) impacts.

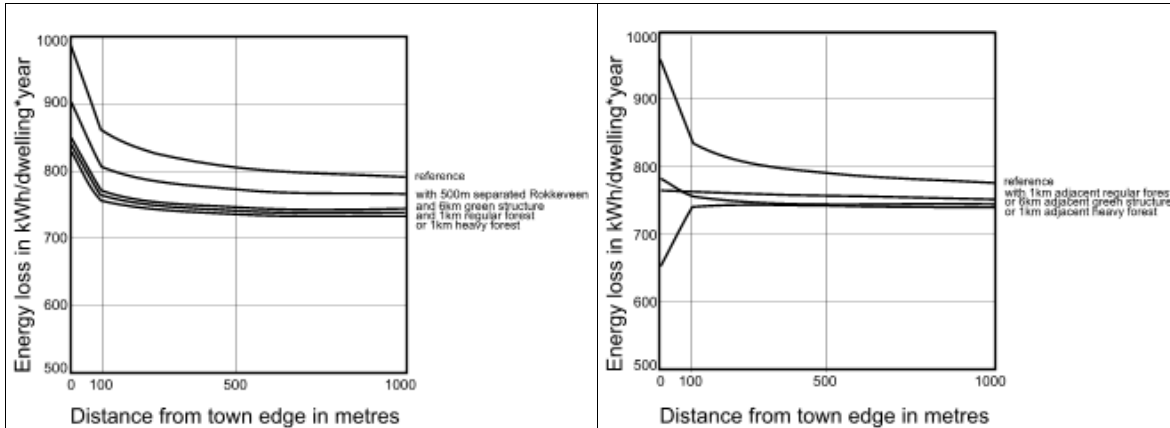


Fig. 275 Impact regional layout on Zoetermeer separated by railways and highway

Fig. 276 Impact locally adjacent shelter on Rokkeveen

Representated impacts are restricted to 1 of 12 wind directions. Figures may be multiplied by a factor 3 to 5 if more directions are sheltered. The impact is decreasing fastly up to 100m in the urban area.

2.4.2 Increase of wind velocity by height

Preceding calculations are tacitly restricted to velocity differences in direction of wind itself (x-direction) and not perpendicular on x (in width y and height z). In Fig. 235 we casually mentioned the importance of velocity differences in height (z-direction), but then the view restricted to a height of 10m (international standard measuring wind) and passing chapter 2.2 to 20m (where wind is not disturbed substantially by single buildings).

On differences in wind velocity perpendicular to wind direction in width (lateral differences in wind velocity) we did not say more than mention them (2.3.4). Tacitly we supposed styled roughnesses and velocities to be continued endlessly perpendicular to the surface of drawing.

However, on this level of scale we can not maintain these simplifications. A separated built up area ('roughness island') undergoes substantial impacts from wind parallel to its edges. Wind survey yielded experimental results by which we can estimate these lateral impacts. However, that requires some insight in increase of wind velocity by height.

To calculate wind velocity v as a working of height z ($v(z)$, wind profile, see Fig. 214, Fig. 278 and Fig. 279) we divide the atmosphere from the largest height $z=d_3$ where wind still is influenced by Earth's surface to the ground in tree layers:

- 90% 'boundary layer' from d_3 to $0.1 \times d_3$;
- 9% 'wall layer' from $d_2 = 0.1 \times d_3$ to $d_1 = 0.01 \times d_3$;
- 1% 'viscose layer' from d_1 to ground level.

The wind velocity of these layers can be approximated by three different formulas (Voorden 1982, Appendix B):

- (1) where $d_3 > z > d_2$: $v_3(z) = v_{d3} \cdot (z/d_3)^\alpha$;
- (2) where $d_2 \geq z \geq d_1$: $v_2(z) = (v_{d3} \cdot 0.4 / (\text{Sqr}(25 + (\ln(d_3 / d_0))^2)) / 0.4) \cdot \ln(z / d_0)$;
- (3) where $d_1 > z > 0$: $v_1(z) = v_2(d_1) \cdot ((2 \cdot z / d_1) - (z^2 / d_1^2))$.

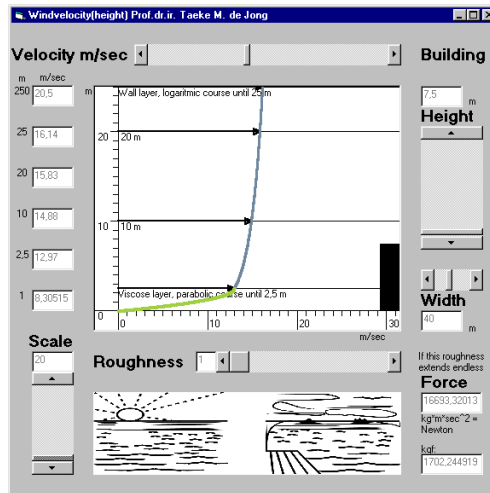
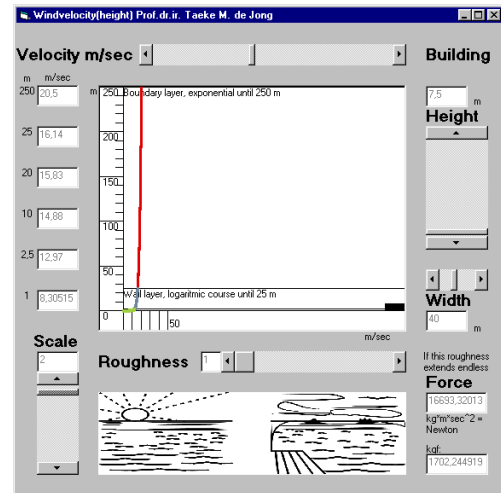
If we know velocity v at d_3 (v_{d3}) the exponential formula (1) produces a velocity for every z in boundary layer below d_3 supposed we know d_3 and exponent α . Exponent α and d_3 are parameters dependent on roughness, we can take them from Fig. 277. For the wall layer the logarithmic formula (2) needs an other parameter d_0 different for every roughness as well (Fig. 277). In an urban environment with much local turbulence the lowest viscose layer has theoretical value only. But for roughnesses lower than 5

we can approximate wind velocities by parabolic formula (3). Within formula (3), formula (2) is used to calculate $v_2(d_1)$.

Rough-ness class	α	d_3	d_2	d_1	d_0	parameters used elsewhere	
						$D(h)$	β
		m	m	m	m		
1	0.104	250	25.0	2.50	0.0002	0	0.07
2	0.144	275	27.5	2.75	0.005	0	0.08
3	0.181	300	30.0	3.00	0.03	0	0.09
4	0.213	350	35.0	3.50	0.1	0	0.11
5	0.245	400	40.0	4.00	0.25	0.3 0.7	0.14
6	0.273	450	45.0	4.50	0.5	0.7	0.16
7	0.313	475	47.5	4.75	1	0.8	0.18
8	0.363	500	50.0	5.00	2	0.8	0.20

Fig. 277 parameters dependent from roughness in formulas used in wind surveys.

If we do not know v_{d3} , but we know v_{10m} or v_{20m} , we can vary the upper scroll bar of the computer programme Windvelocity(height), - downloadable from <http://team.bk.tudelft.nl> publications 2003 - to get the right profile.



Jong (2001)

Fig. 278 Exponential $v_3(z)$ and Logarithmic $v_2(z)$ increase of wind velocity by height

Fig. 279 Logarithmic $v_2(z)$ and Parabolic $v_1(z)$ increase of wind velocity by height

In the logarithmic formula (3) factor $v_{d3} \cdot 0.4 / (\text{Sqr}(25 + (\ln(d_3 / d_0))^2))$ is known as 'wall shearing stress velocity'.

2.4.3 The form of a town

Fig. 280 shows the result of a wind tunnel experiment described in Vermeulen (1986). This experiment serves as a reference for thought experiments to follow.

Above a roughness island like a town or forest in a smooth environment discontinuities in wind velocity appear. The wind meets the edge of the roughness island for the first time ($x = 0$) still having a regular velocity profile like described on page 131. Above the roughness island a specific velocity profile is established with lower velocities than the surrounding smooth surface. However, on some height above the roughness island the old profile remains. The height up to where the new profile establishes its impact is called 'internal boundary layer thickness (Δi)'. The development of this boundary layer is

drawn by dots in Fig. 280. Behind the roughness island the old profile recovers up to a second boundary layer height. In the used model $x=300\text{cm}$ from the first change of roughness, the first boundary layer height (D_1) amounts $16,5\text{ cm}$, the second (D_2) $9,5\text{ cm}$.

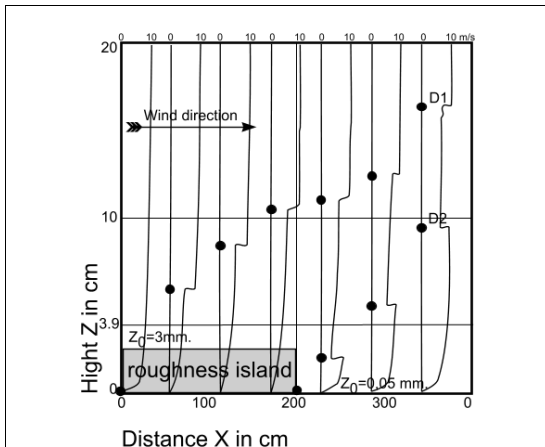


Fig. 280 Wind velocity profiles in height

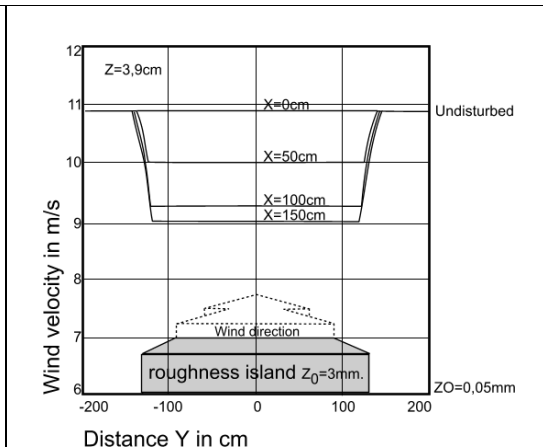


Fig. 281 Wind velocity profiles in width

Fig. 280 shows wind profiles from the beginning ($x=0$) above and behind (up to $x=300$) the roughness island in cross section in case that island would extend endlessly perpendicular to the surface of drawing. Fig. 281 shows wind profiles 3.9cm above the roughness island in front view limited on two sides on a distance of $x=\{0, 50, 100, 150\text{cm}\}$ from the front edge. At $x = 0$ wind still behaves undisturbed like above a smooth surface. After 50cm above the rough surface wind velocity has slowed down, but on both sides the velocity of the smooth surface remains. Between both velocities a lateral transitional zone develops. In the experiment the width of the transitional zone appears to be 1.2 times the internal boundary layer thickness D_1 .

Fig. 280 shows, the thickness of the internal boundary layer D_1 is approximately $1/10$ times the distance to frontal edge x .

So, behind $x=1000\text{m}$ (where D_1 is approximately 100m) a transitional zone can penetrate the air above the roughness island already 120m from the side edges. When the island is 240m width the transitional zones meet each other. So, the wind velocity from this point on could increase by interacting lateral impacts to the back of the island in spite of the underlying roughness.

For example, above an elongated separated urban area with its narrow front to South, Southerly wind not only slows down in its own direction, but produces on the Westerly and Easterly edges a side effect. This increases wind velocity by interaction above the Northern part of the area.

To examine this interaction in more detail a windtunnel experiment on a narrow roughness island is carried out. Fig. 282 shows a map of the model with hypotheses concerning the transition zone, and Fig. 283 a front view with the result of measurements.

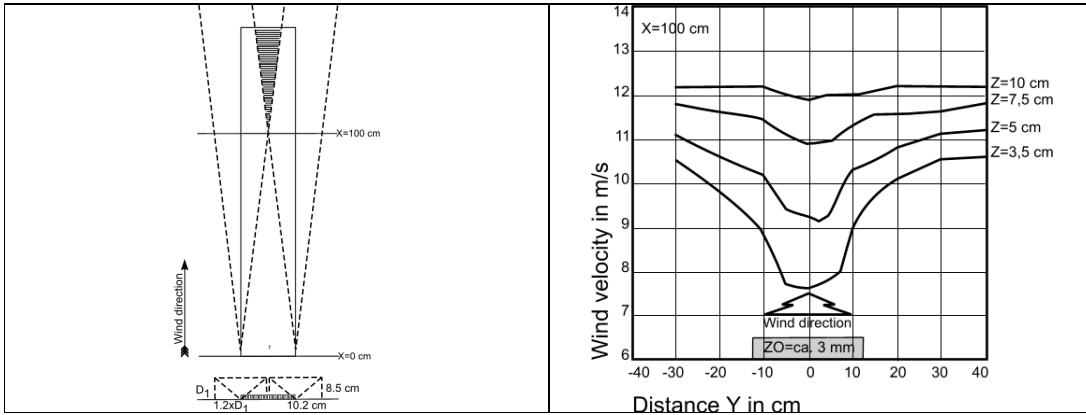


Fig. 282 Hypothetical interaction above an elongated roughness island.

Fig. 283 Measurements above an elongated roughness island $x=100\text{cm}$.

Fig. 283 shows results of measurement near the point where interaction hypothetically should begin ($x=100\text{cm}$). Behind this point (shaded area in Fig. 282) wind velocity should increase anew. Examining these results next deviations draw attention:

- 1 wind velocity decreases more than expected (8,6 m/sec instead of 9,25 m/sec);
- 2 transition zone outside the roughness island is wider than $1,2 \cdot D_1 = 10,2 \text{ cm}$;
- 3 transition zone inside the roughness island is narrower than 10,2 cm.

We can explain these deviations concerning the possibility wind swerves out meeting a narrow roughness island (initial interaction). Fig. 284 represents this additional supposition. As a result of the crooked flow and the material used in the experiment in the very start wind meets a higher roughness than on perpendicular flow. That may explain the first effect. The other effects are caused by a slightly outward initial change of direction of the transition zone as a whole.

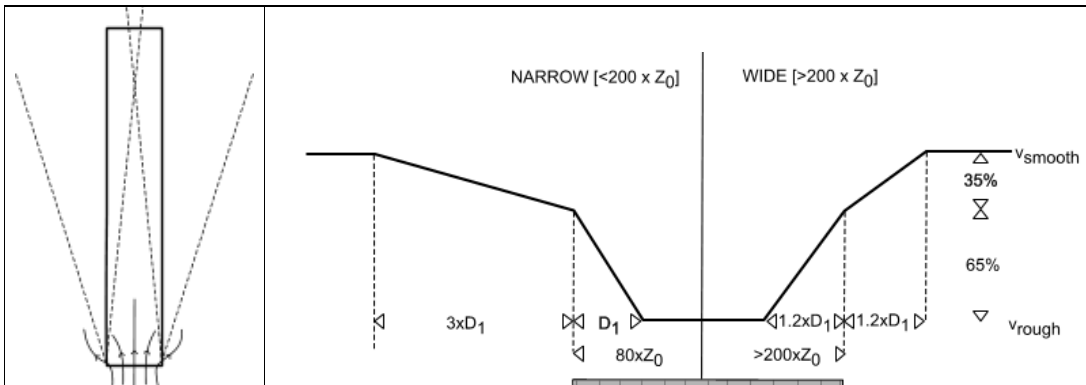


Fig. 284 Supposed initial interaction

Fig. 285 Arithmetical approach of lateral interaction with and without initial interaction

Fig. 285 shows how to calculate wind velocity in transition zones. Starting points are undisturbed velocities above smooth (v_{smooth}) and rough (v_{rough}) surfaces and their internal boundary layer thicknesses d_3 . The difference between both velocities has to be bridged. Above the island already 65 % is bridged, the remaining 35 % is bridged above the smooth surface. A wide roughness island has no initial interaction. The difference is bridged symmetrically in a distance of $1.2 \cdot D_1$. A roughness island narrower than $200 \times Z_0$ (roughness length, not the length of the island) causes initial interaction. Wind velocity difference is bridged over a much larger distance outside the island and above the rough surface over a somewhat smaller distance. The island of Fig. 283 was

25 cm wide, 80 times the roughness length $z_0 = 0,3$ cm, much less than 200. By initial interaction 65 % was bridged above the island over a distance D_1 (8,5 cm), the remaining 35 % over a distance $2 \cdot D_1$ (17 cm).

Returning to the thought experiment of page 125 concerning Leidscheveen we can put Fig. 255 on top of its background Fig. 254 as shown in Fig. 286.

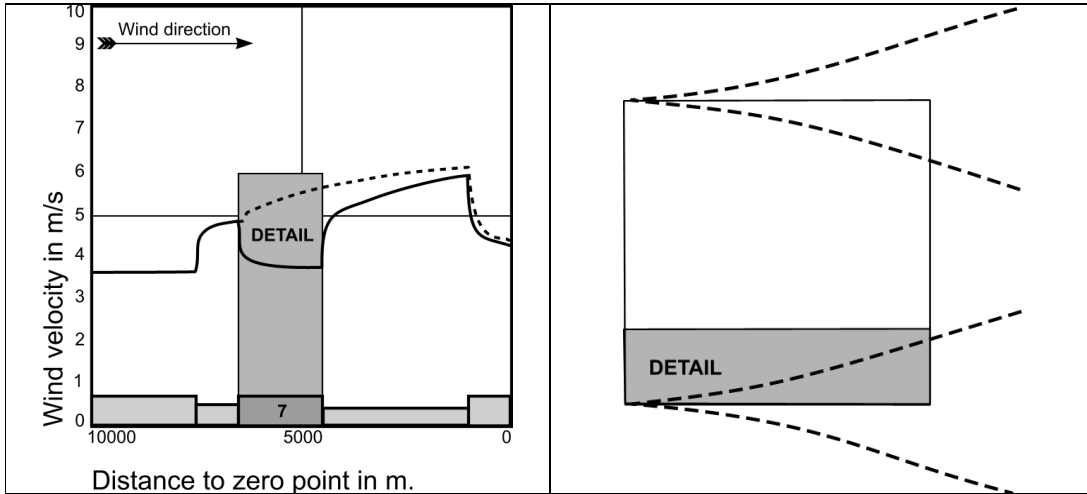


Fig. 286 Westerly wind in and around Leidscheveen from Fig. 254 and Fig. 255

Fig. 287 Leidscheveen as a roughness island

Fig. 287 shows Leidscheveen styled as a square of 2x2km. It has no initial interaction because it is wider than 200 times the roughness length $Z_0 = 1$ belonging to class 7. So, the transition zone will penetrate the built up area $1 \cdot 2 \cdot D_1$ m.

Fig. 288 and Fig. 289 are distorted details of Fig. 286 and Fig. 287.

Fig. 288 shows velocities outside and above Leidscheveen in more detail. Below their difference is represented. 65 % of the difference is bridged above rough urban area (Fig. 288). That is the way you find wind velocity on the edge in between the curves above. In the South East corner of Leidscheveen wind velocity is increased up to 5 m/sec by lateral impacts, while earlier calculations (Fig. 286) indicated there 3,7 m/sec. This velocity is not reached on the East edge until 300 meter ($1 \cdot 2 \cdot D_1$) from the South edge (Fig. 289).

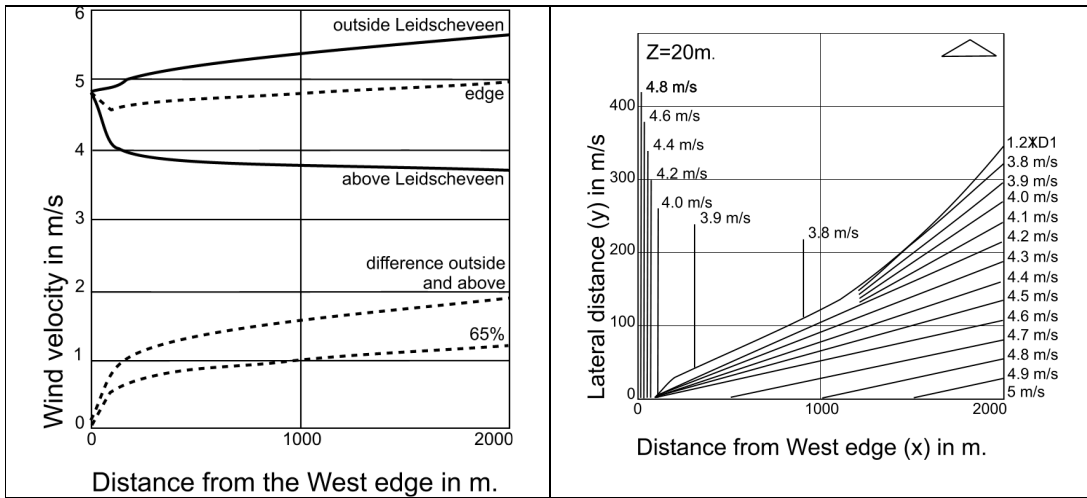


Fig. 288 Given (continues lines) and calculated (dotted) wind velocities outside and above Leidscheveen as distorted detail from Fig. 286

Fig. 289 Transition zone penetrating from South in normal decrease of Westerly wind velocity above Leidscheveen as distorted detail from Fig. 287

From Fig. 280 we learned D_1 (the height where the undisturbed wind velocity meets the disturbed one) is approximately $1/10$ of x . So, we can approximate the distance from the South edge (Fig. 285) $1.2 \times D_1$ in Fig. 289 by drawing a straight line into the South West corner of the island, but here it is calculated according to a method by Vermeulen (1983). From Fig. 288 we know the velocity above Leidscheveen without lateral effect at the East edge (3.7m/sec) and the penetrating velocity in the South East corner (5m/sec). Inbetween the velocity increases proportional (Fig. 285) to the distance from the South edge. The velocities on the South edge we know from Fig. 288 as well. Connecting points of equal wind velocity at the East an South edge we get 'altitude' lines of equal wind velocity.

The below left quadrant of Fig. 290 is a copy from Fig. 289 mirrored 1km above and extrapolated 4km into the East. Width (1km) and length (4km) are not proportionally drawn. Now interaction appears behind the point where $1.2 \cdot D_1$ -lines cross. According to Vermeulen (1986) the 'altitude' lines within the interaction area you can simply connect.

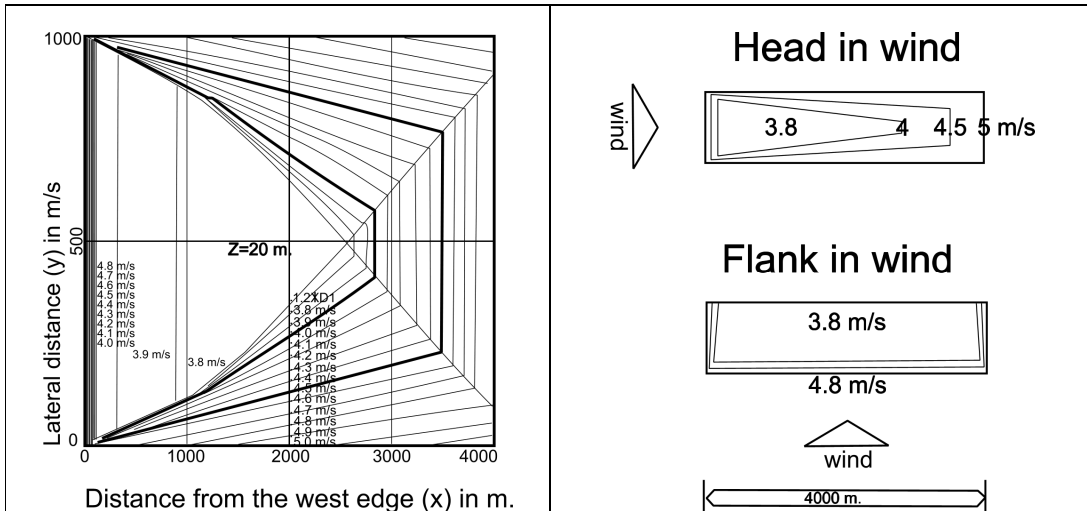


Fig. 290 Elongated island head in wind (length drawn shortened)

Fig. 291 Head and flank in wind (proportionally drawn)

Fig. 291 'head in wind' shows the same model in true proportions: an elongated island with 'altitude lines' 4, 4,5 en 5m/sec adopted from Fig. 290. Wind velocity in heart line primarily drops from 4.8 to 3.8m/sec, but then increases up to 5m/sec on the East edge due to lateral impacts. Drawing the case 'flank in wind' the first left km from Fig. 290 is used only extrapolating the middle parts. In that case the urban area is surprisingly exposed to lower wind velocities because lateral impacts play practically no rôle. That conclusion is controversial to the usual intuition that elongated urban areas should be located with 'head in wind'. 'Flank in wind' appears to be better from a viewpoint of shelter. However, the question is how much this measure yields. Fig. 292 compares them by a grid of hectares.

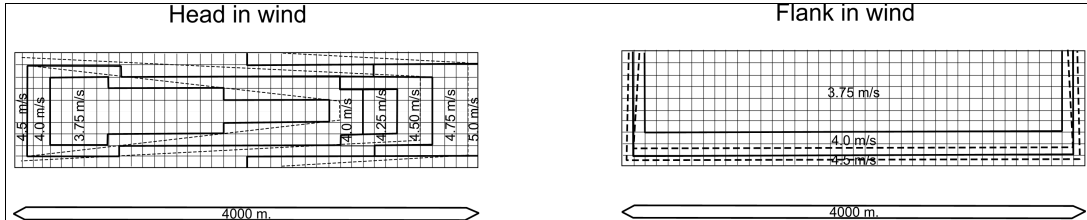


Fig. 292 Wind velocities per hectare

Suppose there are 40 dwelling per hectare. From ventilation losses of non airtight dwellings due to Westerly wind we now can calculate the total difference.

Windvelocity	head	flank	Ventilation loss in kWh due to Westerly wind			
m/sec	ha	ha	Per dwelling	Per ha.	Total head	Totaal flank
3,75	88	252	504	20160	1774080	5080320
4,00	98	90	521	20840	2042320	1875600
4,25	12		539	21560	258720	
4,50	120	58	557	22280	2673600	1292240
4,75	34		577	23080	784720	
5,00	48		597	23880	1146240	
Totaal	400	400			8679680	8248160

Fig. 293 Difference in ventilation loss head and flank in wind

The difference due to western wind amounts $8679680 - 8248160 = 431\ 520$ kWh per year (approximately 27 kWh average per dwelling). However, this amount can not be charged as profit by giving an elongated urban area a turn by 90° . On every orientation after all, the impact of at least four wind directions have to be analysed. Then the profit is the difference in impact from two wind directions head and two flank.

2.4.4 Dispersion of urban area

Is a non elongated ('compact') town better than a whether or not favourably oriented elongated or dispersed one? This question can not be answered for all cases because elongatedness is substantially dependent from orientation. Anyway, for Westerly wind in case of Leidscheveen the following is valid. Fig. 294 and Fig. 295 show three classes of wind velocity on a hectare grid.

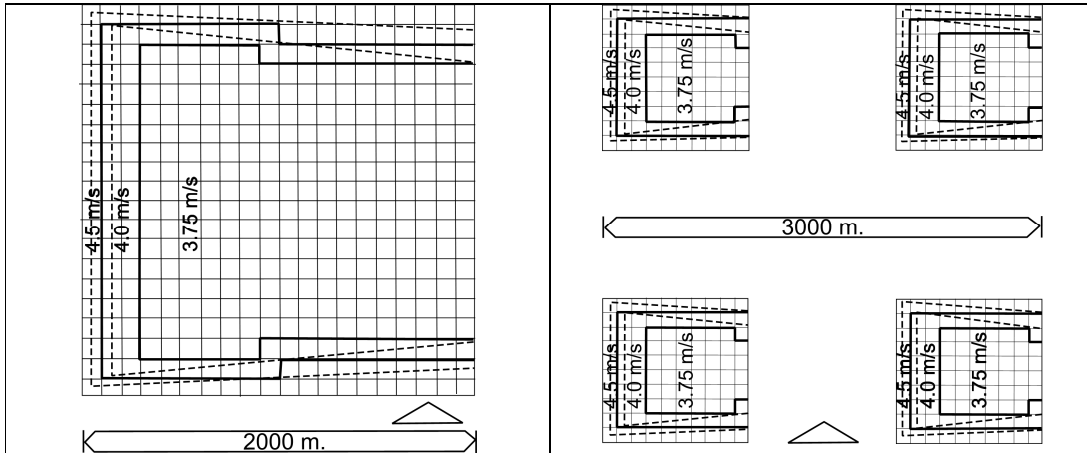


Fig. 294 Compact town

Fig. 295 Dispersed town

From the ventilation loss per dwelling due to Westerly wind of 3,75, 4 en 4,50 m/sec we can calculate a difference (Fig. 296).

Windvelocity m/sec	Spread		Ventilationloss in kWh due to westerly wind			
	Compact ha	Spread ha	per woning	per ha	totaal compact	totaal gespreid
3,75	250	160	504	20160	5040000	3225600
4,00	72	128	521	20840	1500480	2667520
4,50	78	112	557	22280	1737840	2495360
Totaal	400				8278320	8388480

Fig. 296 Difference in ventilation loss in compact and dispersed towns

The difference in favour of building compact towns amounts $8388480 - 8278320 = 110\ 160$ kWh per year only (approximately 7 kWh average per dwelling). Velocity and probability of Western wind amounts a little above the average. So, you can multiply this figure by approximately 10 to estimate the total profit.

Comparison with elongated forms is more difficult by orientation sensitivity. A fast method of multiplying the profit of westerly wind does not make sense then. For every several case the calculation has to be repeated for all 12 wind directions. We will not elaborate that.

The intended profit of this paragraph to be used in next paragraphs is insight in the importance of lateral wind effects as such.

2.4.5 The form of town edge

The acquired insights make rough study of town edge design possible. By doing that in the same time we reach the lowest level of scale roughness based calculations can be useful. On lower levels of scale the average image of roughness is disturbed too much by local form variations essential for urban design. However, they remain indispensable as input for predictions on lower levels of scale. The next chapter will examine levels of district and neighbourhood further by carefully designed wind tunnel experiments. They will link up connections between urban design and wind behaviour in more detail.

However, on the level of town edge design the roughness approach (grain approximately 100m radius) still makes sense for rough conclusions. We restrict to the impacts of large gaps in the city edge. They occur by large access roads with noise zones or green lobes penetrating the city.

Fig. 297 shows a model of a small town (approximately 50 duizend inwoners) with lobes like that.

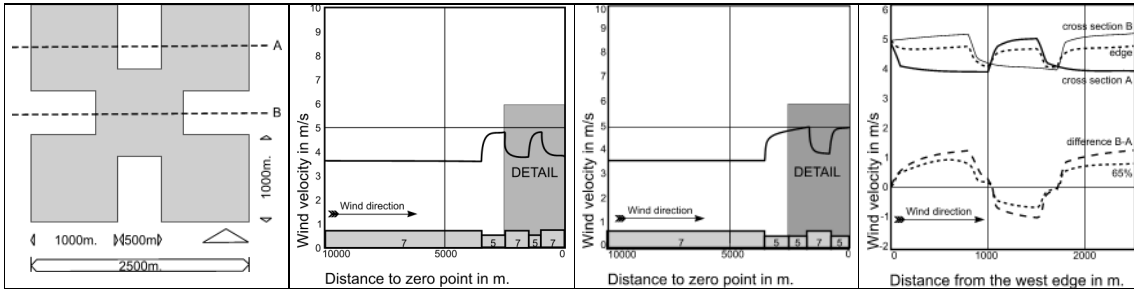


Fig. 297 Small town with green lobes

Fig. 298 Wind velocity profile cross section A

Fig. 299 Windvelocity profiel doorsnede B

Fig. 300 Difference profile A en B

Fig. 298 and Fig. 299 show the windvelocity profiles of cross section A and B in case it would be Leidscheveen blown by Western wind. Fig. 300 shows above the last 3000m of both profiles projected on top of eachother. Below the difference between both profiles is represented; 65% has to be bridged laterally above urban area over a distance $1,2 \cdot D_1$. This determines wind velocity on the edge.

From these data we estimate again an average wind velocity per hectare.

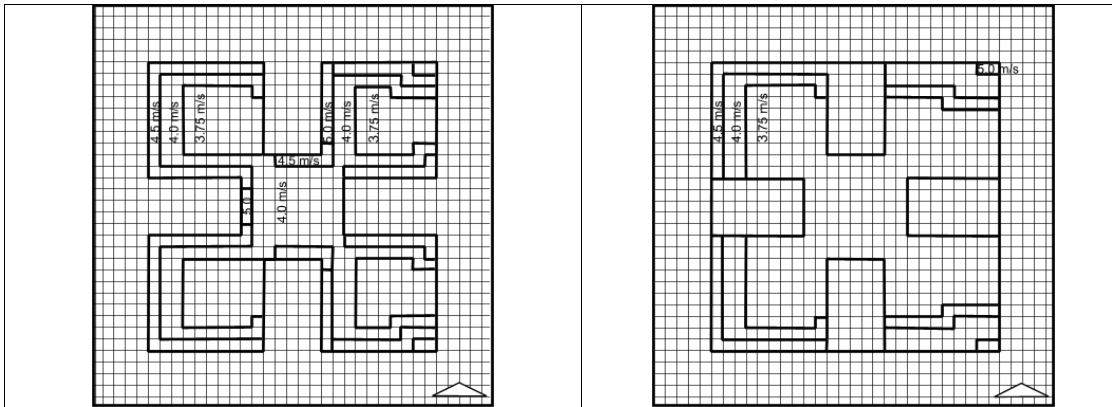


Fig. 301 'Open' towns edge

Fig. 302 'Closed' towns edge

Fig. 301 shows lobes penetrating from four directions. In Fig. 302 the lobes are filled with forest of the same roughness as the urban area keeping the urban surface equal. From the ventilation losses belonging to wind velocity 3,75, 4, 4,5 and 5m/sec due to westerly wind, Fig. 303 calculates the difference.

Windvelocity m/sec	Open ha	Closed ha	Ventilationloss in kWh due to westerly wind			
			per dwelling	per ha	total open	total closed
2,75	154	305	504	20160	3104640	6148800
4,00	184	74	521	20840	3834560	1542160
4,50	106	82	557	22280	2361680	1826960
5,00	21	4	597	23880	501480	95520
Totaal	465	465			9802360	9613440

Fig. 303 Difference in ventilation loss by 'open' and 'closed' town edge

The difference is $9\ 802\ 360 - 9\ 613\ 440 = 188\ 920$ kWh per year (Approximately 10 kWh per dwelling). Multiplying Westerly wind impact by 10 the total average profit is approximately 100 kWh x 1860 dwellings.

2.4.6 Wind directions, temperature and built form

In chapter 2.2 we restricted our thought experiments to two wind directions and in this chapter even to one (Westerly wind). Assuming an average temperature for all wind directions we reported virtual ventilation losses of non airtight, low rise buildings due to Westerly wind as an indicator. Their differences clarified an impact of environmental roughness useful for other impacts as well. We exclusively varied regional and local environment applying different roughnesses, keeping the rest constant. Otherwise the impact of environmental roughness on itself could not be clarified. It would be mixed up with other causes (possible measures). To clarify other causes the reverse we have to keep environmental roughness constant. If we take one layout of roughnesses in the environment – the one we will use in next chapters for experiments in the wind tunnel (Fig. 308) – we can compare the contribution of every several wind direction and their temperature properly (Fig. 304). We calculated energy losses by ventilation for every wind direction in the same way we did above (column A and B) and for airtight dwellings (column C and D).

		without temperature influence				temperature influence		with temperature influence			
		non airtight		airtight		non airtight	airtight	non airtight		airtight	
wind direction		A	B	C	D	E	F	A x E	B x E	C x F	D x F
'hours'	degrees	kWh		kWh				kWh		kWh	
1	30	322	6%	154	6%	70%	66%	227	4%	101	4%
2	60	492	9%	228	9%	116%	111%	570	10%	254	10%
East	3	405	7%	201	8%	168%	151%	681	12%	304	12%
	4	246	4%	129	5%	205%	174%	504	9%	225	9%
	5	369	7%	186	8%	64%	57%	238	4%	106	4%
South	6	530	10%	259	10%	71%	65%	377	7%	168	7%
	7	729	13%	232	9%	100%	141%	731	13%	326	13%
	8	769	14%	315	13%	107%	116%	819	15%	365	15%
West	9	591	11%	253	10%	107%	111%	631	11%	281	11%
	10	389	7%	172	7%	90%	91%	349	6%	156	6%
	11	366	7%	173	7%	71%	67%	260	5%	116	5%
North	12	329	6%	167	7%	45%	40%	149	3%	67	3%
	Total	5537	100%	2469	100%			5536	100%	2469	100%

Fig. 304 Contributions per wind direction to total energy loss by ventilation

In the lowest row 'Total', column A shows we can multiply the loss of Westerly wind by 10 to have an idea of total loss from all directions indeed. The totals without temperature influence are the same as those including temperature influence, because in columns A, B, C and D we assumed an average temperature of all directions.

Columns E and G show tentative weight factors for temperature, based on Visser (1986). Multiplying A, B, C and D by these factors produces the necessary correction to get a better idea about the real losses per direction. They are used in next chapters as well.

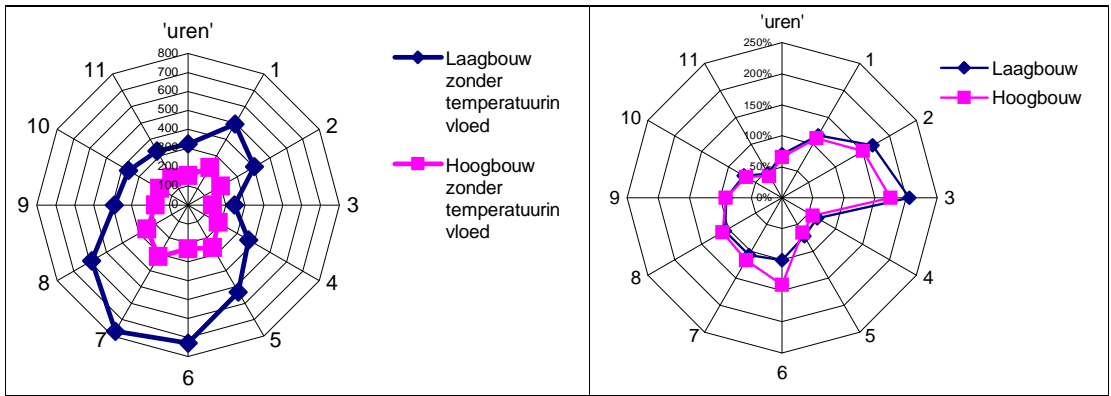


Fig. 305 Contributions per wind direction to total energy loss by ventilation without temperature influence (A and C in Fig. 304)

Fig. 306 Tentative correction factors for temperature influence (E and F in Fig. 304)

Fig. 305 and Fig. 306 show Easterly winds being less probable but colder have a larger impact on energy losses by ventilation than South Westerly winds. To understand why Southerly winds contribute more in airtight buildings (Hoogbouw in Fig. 306) than in non airtight ones (Laagbouw) you have to look at Fig. 221.

2.5 District and neighbourhood variants

2.5.1 From calculable 'rough surface' into allotments in a wind tunnel

Changing location and size of a homogenous undirected roughness, influences every external wind direction in the same way. However, changing form on a lower level of scale introduces internal directions within that field of roughness behaving differently even for one single external wind direction. And design can vary form within form. This complication you can imagine as 3 potter's wheels turning around the same centre. If we consider 12 directions, there are 12 x 12 x 12 combinations (Fig. 307).

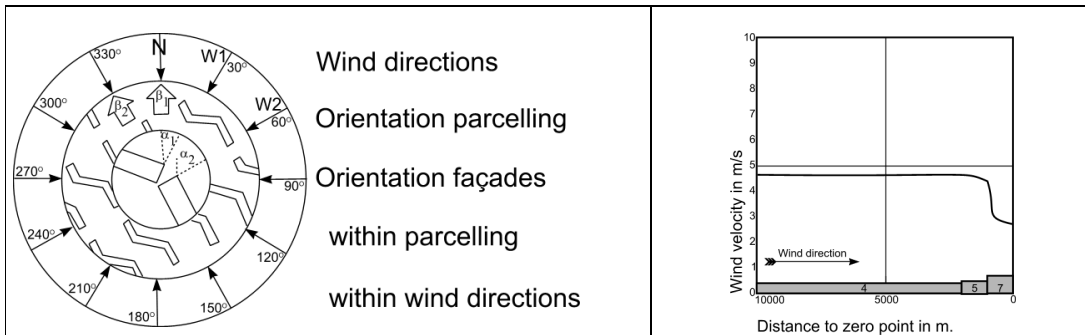


Fig. 307 Three levels of schale where orientation has to be taken into account

Fig. 308 Supposed wind tunnel context by standard Northerly wind

The external wheel represents 12 local wind statistics (W1, W2, W3 ... concerning probability, velocity and temperature) as it applies outside and at the edge of the urban fragment we consider. The second wheel represents the considered fragment with its own arrow indicating North (β_1). In this chapter the direction of the allotment as a whole ($\beta_1, \beta_2, \beta_3 \dots$) is variable. The middle wheel represents façades within the allotment having variable orientations ($\alpha_1, \alpha_2, \alpha_3 \dots$), causing different ventilation losses locally. In previous paragraphs α and β were neglected. Ventilation losses were averaged over all directions of allotments and façades.

In this chapter α and β are varied by interpreting tests of 18 different allotments in the wind tunnel of Visser (1986) from 7 different angles ($0^\circ - 90^\circ$ by steps of 15°) with a standardised W and foreland roughness (Fig. 308). From these 7 measured angles, 4 ($0^\circ - 90^\circ$ by steps of 30°) appeared to be sufficient to draw conclusions about all directions of allotment.

2.5.2 Wind tunnel experiments

On the level of districts and neighbourhoods 4 configurations 1 x 1 km Jong (1986) - fully elaborated in models 1:500 - are tested by Visser (1986). In each of the four models 30 x 2 measuring points were installed at front and back side of different building blocks to measure pressure differences (Fig. 309).

Right above in each configuration (Fig. 309) each time you find a quarter of a district centre. So, any configuration could be thought mirrored twice around this centre into a full district 2x2km consisting of 4 district quarters. Each configuration consists of 9 neighbourhood quarters 300x300m (one central, 8 peripheral). Each neighbourhood quarter consists of 9 ensemble quarters (hectares 100x100m one central, 8 peripheral). District roads are planted with trees; neighbourhood and ensemble roads are not.

The configuration is outside blown along from North to East (90° from North). At South and West side the configuration as a district quarter is part of an imaginary district filled up with equal roughness. In this paragraph we study the differences between the four configurations not trying to develop calculation models.

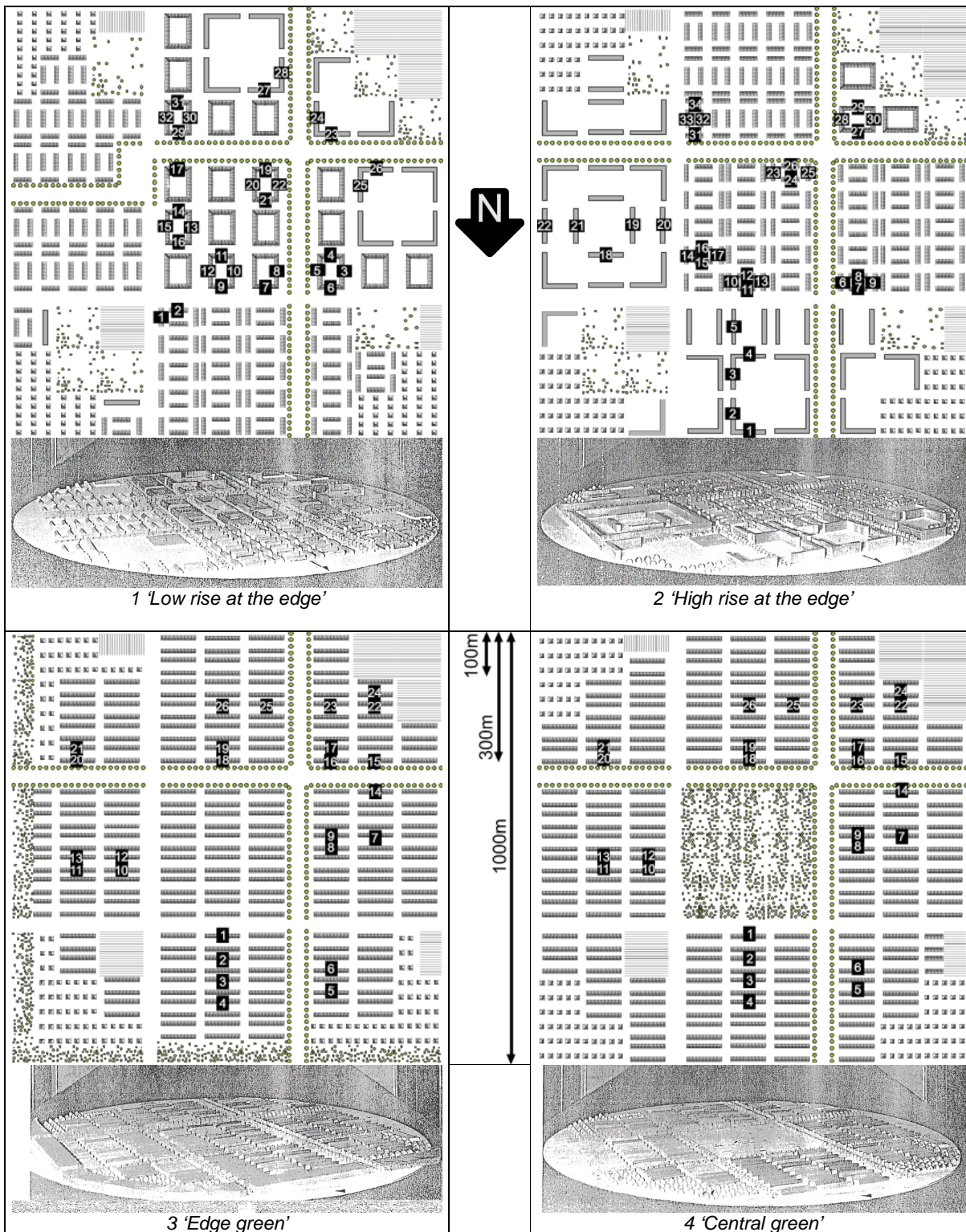


Fig. 309 District configurations in wind tunnel with measuring points indicated

Concerning the average result of all measuring points the differences between the configurations are remarkably small. However, there are substantial differences between locations within configurations. (Fig. 316 and Fig. 319). Fig. 310 shows hectare allotments applied in the tested configurations.

In configuration 1 and 2				
	Vrije sect. 30w/h 10m	Hoek1a 22w/ha 22m	Hof1 96 w/ha 15,5m	Hof4 53,3w/h 10m
In configuration 2			In configuration 3 and 4:	
	Lijn10 84w/ha 17m			Lijn12 53w/ha 10m

Fig. 310 Hectare allotments applied in the tested configurations

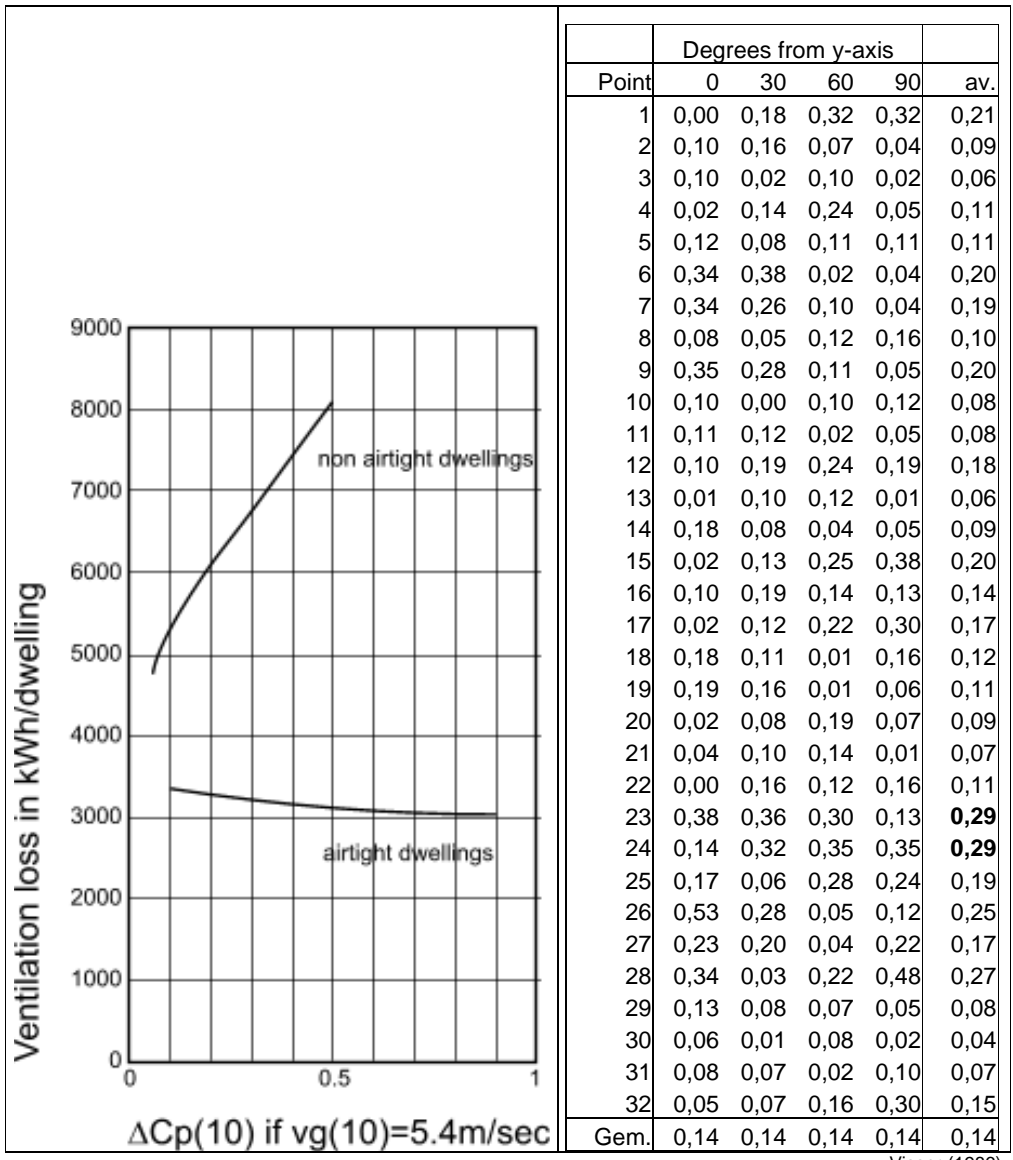
In paragraph 2.6.1 we study the results of 14 wind tunnel experiments by Visser (1986) on hectare level; 7 with green and 7 without. In these experiments a number of theoretical repeating point, line, corner and courtyard allotments 500x500m elaborated in models 1:250 are tested. The force these allotments undergo by standard wind is measured. From these tests TNO developed a calculation method for allotments repeating in two dimensions. By this method more types of allotment are calculated.

2.5.3 Pressure differences between front and back façades

Ventilation loss of a dwelling not only depends on wind statistics derived from year average wind velocity v_g on $z=10m$ height in the nearest wind measuring station ($v_g(10)$, for example 5,4m/sec near Schiphol). It depends also on the environment and orientation of the building block. On these more local factors pressure differences between front and back façades follow determining ventilation losses at last.

Pressure differences are proportional to driving pressure of wind: $0,5 \times \rho \times v_g(10)^2$. In this formula ρ ('ro') is the density of air. Pressure differences between front and back façades determining ventilation are measured in wind tunnel. Dividing such pressure differences by the local driving pressure of wind produces a factor $\Delta C_p(10)$ representing the resistance of an allotment independent from wind velocity. The result of wind tunnel tests are expressed in $\Delta C_p(10)$. Fig. 311 shows the relation between ventilation loss near Schiphol and $\Delta C_p(10)$ in any wind direction Visser (1986). Airtight buildings in $v_g(10)$ lose less energy by increasing pressure because inhabitants close windows they opened in less pressure!

Inside urban areas energy yield of wind turbines is less relevant. However, pressure difference is important as well for comfort of outdoor space, dispersion of air pollution and wind loads. But we have measured ventilation losses and will use it as an indicator.



Visser (1986)

Fig. 311 Ventilation loss related to $\Delta C_p(10)$ if $v_g(10) = 5,4m/sec$

Fig. 312 $\Delta C_p(10)$ in measure points of configuration 1 in 4 directions

Fig. 312 shows $\Delta C_p(10)$ measured in every measure point of configuration 1 four times while wind was blowing 0° to 90° from y-axis each time turning the model 30° (any direction could be North). Measuring points 23 and 24 (high rise at a crossing, see Fig. 309 conf. 1) suffer the largest pressure differences, 23 on 0° , 24 on 60° and 90° . This kind of details we study in paragraph 2.5.5. This paragraph studies the averages in lowest row compared with the averages of the other configurations.

2.5.4 District lay out

The averages in lowest row of Fig. 312 seem to show the direction of wind does not matter but this is only the case in configuration 1. It is explained best because half of the measured blocks there are oriented perpendicular to the other half. So, the minimum ventilation loss of one building block compensates the maximum of the other one. Configuration 2 is less balanced that way and configurations 3 and 4 have only one orientation of building blocks (Fig. 313).

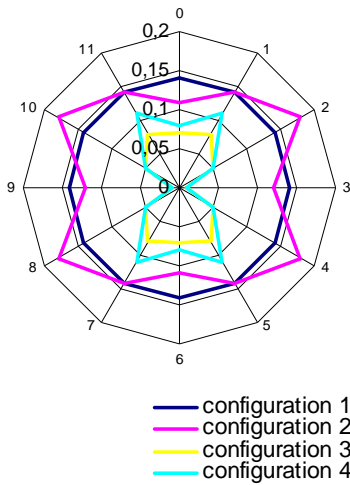


Fig. 313 Average $\Delta C_p(10)$ in different configurations two times mirrored around the centre.

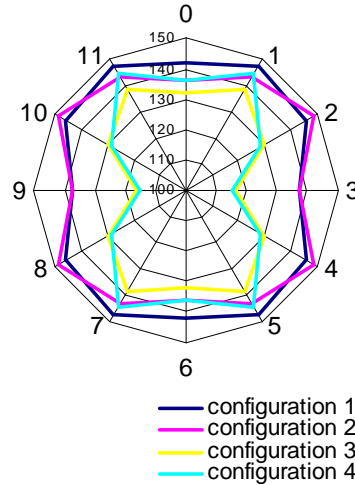


Fig. 314 Average ventilation loss of a non airtight dwelling in kWh per allotment direction if standard Northerly wind would blow from all directions

Comparing the impact of locations and allotment directions we should use an equal standard wind (here Northerly wind, representing approximately 2.69% of the virtual total ventilation loss per allotment direction) for every allotment direction (Fig. 314). The virtual total ventilation loss then is 100%. Fig. 315 shows averages multiplied into such a virtual total. In configuration 1 it is 5 344 kWh for non airtight dwellings. That is less than we calculated by roughness 7 in Fig. 304 (5 536 kWh in column A X E), and for airtight dwellings it is more (3 266 kWh instead of 2 469 in column C x F). Perhaps the roughness class of configurations is closer to 8 than class 7 we used in paragraph 2.4.6 and supposed in Fig. 308.

	Configuration 1			Configuration 2		Configuration 3		Configuration 4	
	calculated								
	roughness	average	virtual	average	virtual	average	virtual	average	virtual
	100%	2,69%	100%	2,69%	100%	2,69%	100%	2,69%	100%
non airtight	5536	144	5344	141	5233	129	4787	131	4862
airtight	2469	88	3266	89	3303				
$\Delta C_p(10)$		0,14		0,14		0,05		0,06	

Fig. 315 Estimating average ventilation losses from 4 allotment directions multiplied into a virtual total.

Average pressure difference in configuration 2 (high rise on the edge) is the same ($\Delta C_p(10)=0.14$) as in configuration 1 (low rise on the edge). But there are differences per allotment direction. So, you can not yet conclude both configurations should have the same ventilation loss. Wind directions deliver different contributions and their reduction depends on the North direction arrow of the allotment in the compass card of wind directions. Because configuration 3 (edge green) and configuration 4 (central green) have lower pressure differences in all directions (Fig. 314) we can conclude they will have less ventilation loss than configurations 1 and 2 indeed. However, the difference between a lay out with green on the edge or within the centre is negligible!

Configuration 1 (low rise on the edge) has more ventilation losses from non airtight low rise dwellings and less from airtight high rise ones than configuration 2 (high rise on the edge). Fig. 311 shows airtight highrise has less ventilation loss by more wind pressure. Inhabitants close their windows earlier.

Slant flow along (30° of 60°) causes in all cases maximum loss (Fig. 313). Perhaps we should orientate allotments with two perpendicular directions East or South West sheltering one of them best and the other not at all. This yields more than both half. We tested that hypothesis by calculating perpendicular and slant flowing along for 12 North direction arrows but the result disappointed because adjacent wind directions score high as well by slant flow. They dim the aimed impact into a negligible result.

That is of course not the case in parallel blocked configurations 3 and 4.

So, measures on the level of district or neighbourhood have more local than general impacts. Big local impacts level out in the district as a whole in such a way that differences in its layout become marginal.

2.5.5 Neighbourhoods

We restrict ourselves to perpendicular flow with Northerly wind character (2.7%) from 0° and 90° out of y-axis. In both cases wind meets on 300m from town edge a 30m wide neighbourhood road and on 600m a 70m wide district road with trees.

A roughness approach (paragraph 2.4.6) would show decreasing loss until 100m from town edge stabilising on approx. 150kWh for non airtight low rise and for airtight high rise increasing stabilising on 75 kWh. Fig. 316 shows wind tunnel results elaborated into kWh (paragraph 2.4) from configurations 1 (low rise on the edge) and 2 (high rise on the edge) as a working of distance to town edge.

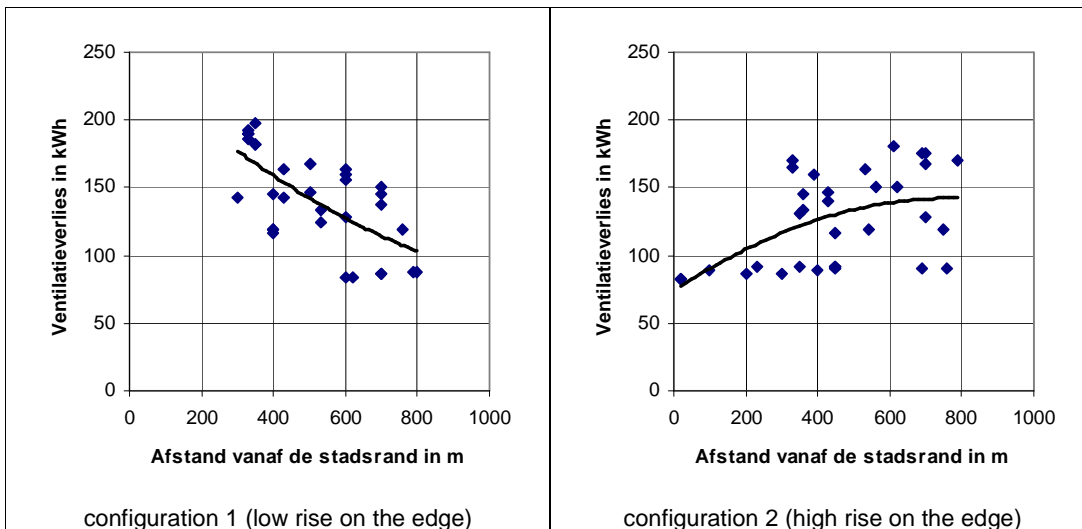


Fig. 316 Ventilation losses of non airtight low rise and airtight high rise dwellings by standard Northerly wind (2.7% of virtual total) as a function of distance to town edge in configurations 1 and 2

Wind tunnel experiments now specified to location give a clearer distinction between low rise and high rise on the edge then leveled out over the district. The largest low rise loss in configuration 1 appears in measure point 15 (197kWh), a 15.5m high building located on a 15m wide road without trees and a foreland of 10m high dwellings. The smallest appears in measure point 13 (116kWh), a courtyard dwelling. The difference is approx. 80 or virtually 3000kWh.

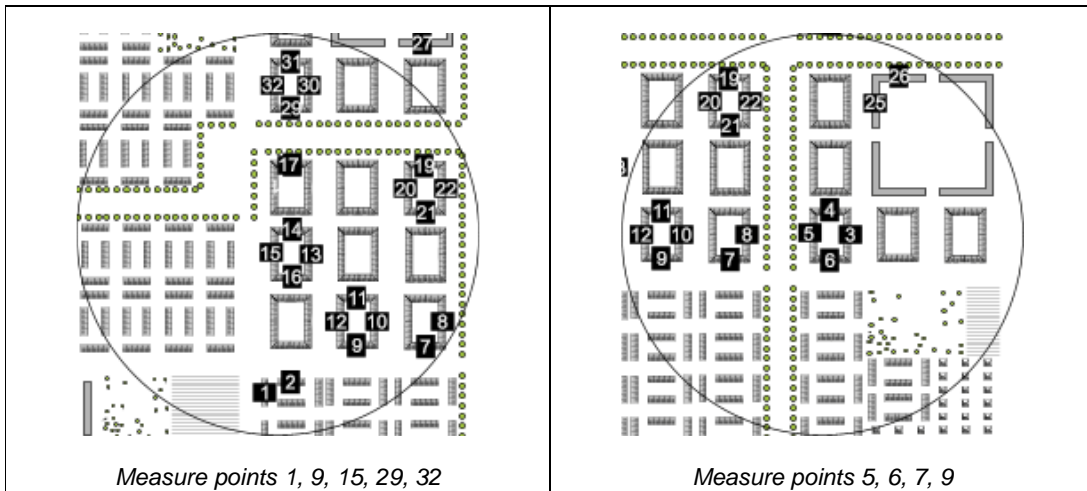


Fig. 317 Measure points in configuration 1 in a radius of 300m

Measure points 1(186kWh), 6(190kWh), 7(190kWh), 9(163kWh), 15(197kWh) and 32(182kWh) score high by wind over a 40m neighbourhood road without trees. Measure points 5(145kWh), 17(143kWh) and 29(150kWh) get wind over a much wider district road (80 to 100m) with 6m high trees. The local importance of trees in large urban spaces is indicated here. The difference is approx. 40 or virtually 1500kWh.

In configuration 2 measure points 7(147kWh), 11(170kWh) en 14(131kWh) lie on a 40m wide neighbourhood road without trees. Measure point 14 scores low because it is sheltered by 22m high high rise buildings on the other side of the road. The low rise minimum measure point 10(116kWh) lies on 10m wide ensemble streets. The maximum in measure point 25(180kWh) is most likely explained by its position on the edge of the used model.

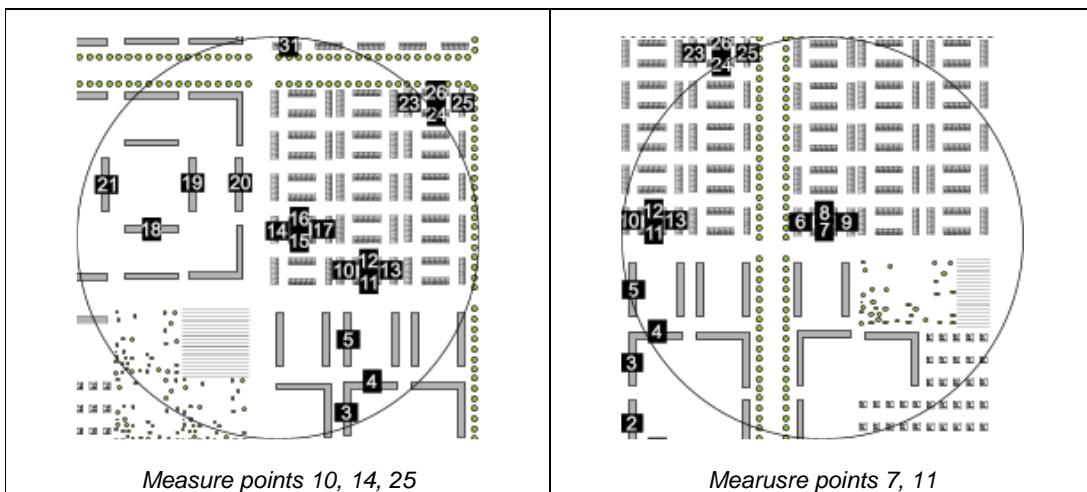


Fig. 318 Measure points in configuration 2 in a radius of 300m

Fig. 319 shows the same figures as Fig. 316 for configuration 3 en 4 without high rise.

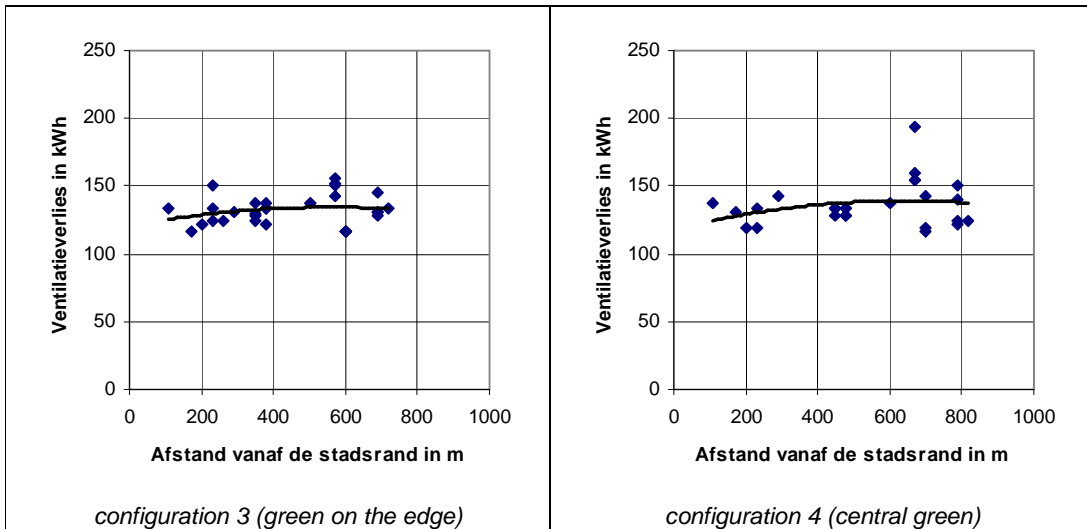


Fig. 319 Ventilation losses of non airtight low rise dwellings by standard Northerly wind (2.7% of virtual total) as a function of distance to town edge in configurations 3 and 4

In configuration 3 measure point 27(150kWh) lies on a 40m wide neighbourhood road without trees. Measure points 20(156kWh), 18(152kWh), 15(150kWh) and 16(143kWh) score approximately equally high lying on a 70m wide district road with trees. Minima 2(116kWh), 17(116kWh), 19(116kWh) and 21(116kWh) get wind from a backyard lying on 10m wide ensemble roads.

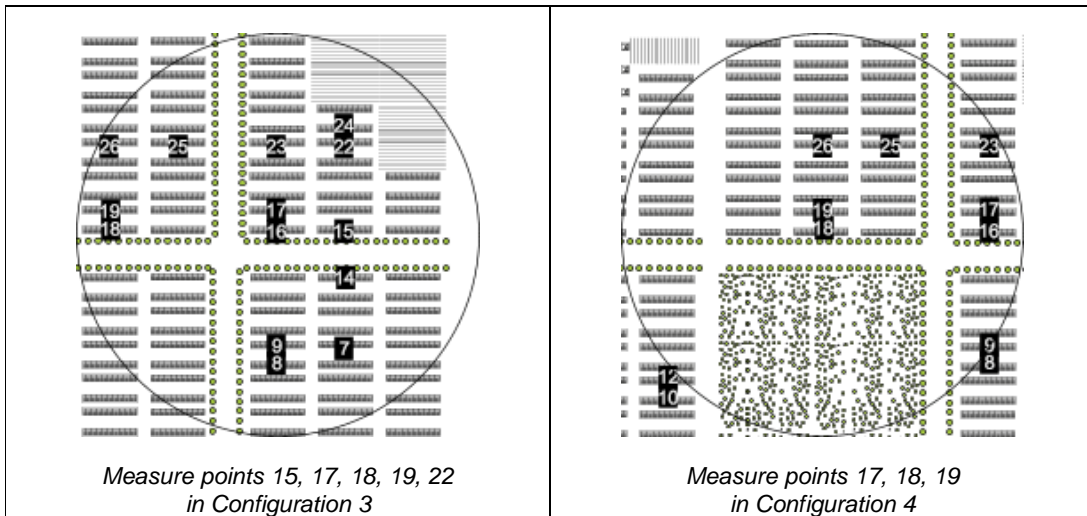


Fig. 320 Measure points in configuration 3 and 4 in a radius of 300m

In configuration 4 measure point 18(194kWh) scores extremely high. It gets wind from 300m wide open green area in the centre of district quarter. Even district road trees do not help much on this location. Minima 21(116kWh), 6(119kWh), 5(119kWh) and 17(119kWh) again lie on small ensemble streets. Measure point 19(143kWh) lies on a small street as well, but that is the first street behind the green behind measure point 18(194kWh), and that is still apparent there.

2.6 Allotment of hectares

2.6.1 From wind tunnel experiments into methods of calculation

From the results of 14 wind tunnel experiments on repeating theoretical point, line, corner and courtyard allotments with and without green a calculation method is developed Visser (1987; Visser (1987) predicting average pressure differences between front and back façades of dwellings $\Delta C_p(z)$ (ΔC_p on height z). The reference height z is 2.5 times the average building height.

The calculation is restricted to allotments with two main directions at most. For two directions we have to determine the value of ΔC_p perpendicular blown along by wind (ΔC_{p0}). Façades may bend 30° from main direction at most. Within that margin measuring a second main direction is not necessary. The expected ΔC_p per flow direction is calculated for 100 x 100m allotment types in Fig. 321.



Visser (1987; Visser (1987)

Fig. 321 Allotment types 100x100m with different height Visser (1987) calculated $\Delta C_p(z)$ for

Fig. 322 shows the result of these calculations.

WIND, SOUND AND NOISE ALLOTMENT OF HECTARES FROM WIND TUNNEL EXPERIMENTS INTO METHODS OF CALCULATION

	height	vert.surf.	without green					with green 6m high					with green 10m high				
	m	F/O	N	+30	+60	+90	av.	N	+30	+60	+90	gem.	N	+30	+60	+90	av.
Punt01	10	0,24	0,14	0,13	0,09	0,00	0,09	0,13	0,12	0,09	0,00	0,09	0,12	0,11	0,08	0,00	0,08
Punt02	10	0,24	0,14	0,13	0,09	0,00	0,09	0,13	0,12	0,09	0,00	0,09	0,12	0,11	0,08	0,00	0,08
Punt03	10	0,24	0,19	0,17	0,13	0,00	0,12	0,18	0,17	0,12	0,00	0,12	0,12	0,19	0,11	0,00	0,11
Punt05	10	0,16	0,19	0,17	0,12	0,00	0,12	0,18	0,17	0,12	0,00	0,12	0,12	0,19	0,11	0,00	0,11
Punt06	10	0,30	0,14	0,13	0,10	0,00	0,09	0,14	0,13	0,09	0,00	0,09	0,13	0,12	0,08	0,00	0,08
Punt07	15,5	0,14	0,23	0,21	0,15	0,00	0,15	0,22	0,20	0,14	0,00	0,14	0,20	0,19	0,13	0,00	0,13
Punt08	15,5	0,21	0,16	0,15	0,11	0,00	0,11	0,16	0,14	0,10	0,00	0,10	0,14	0,13	0,03	0,00	0,08
Punt09	22	0,09	0,20	0,19	0,13	0,00	0,13	0,20	0,10	0,10	0,00	0,10	0,20	0,19	0,13	0,00	0,13
Punt10	22	0,18	0,19	0,18	0,13	0,00	0,13	0,19	0,18	0,10	0,00	0,12	0,18	0,12	0,12	0,00	0,11
Lijn01	10	0,24	0,21	0,19	0,14	0,00	0,14	0,20	0,18	0,13	0,00	0,13	0,18	0,12	0,12	0,00	0,11
Lijn02	10	0,24	0,21	0,19	0,14	0,00	0,14	0,20	0,19	0,13	0,00	0,13	0,18	0,17	0,12	0,00	0,12
Lijn05	10	0,32	0,14	0,13	0,03	0,00	0,08	0,13	0,12	0,08	0,00	0,08	0,12	0,11	0,09	0,00	0,08
Lijn06	15,5	0,25	0,20	0,19	0,13	0,00	0,13	0,19	0,18	0,10	0,00	0,12	0,18	0,16	0,12	0,00	0,12
Lijn07	11	0,18	0,28	0,26	0,18	0,00	0,18	0,27	0,24	0,18	0,00	0,17	0,24	0,22	0,16	0,00	0,16
Lijn08	22	0,35	0,12	0,11	0,08	0,00	0,08	0,12	0,11	0,08	0,00	0,08	0,11	0,10	0,07	0,00	0,07
Lijn09	22	0,35	0,12	0,11	0,08	0,00	0,08	0,12	0,11	0,08	0,00	0,08	0,11	0,10	0,07	0,00	0,07
Hoek01	22	0,18	0,28	0,26	0,18	0,00	0,18	0,28	0,26	0,18	0,00	0,18	0,27	0,24	0,19	0,00	0,18
Hoek02	22	0,35	0,28	0,26	0,18	0,00	0,18	0,28	0,26	0,18	0,00	0,18	0,27	0,24	0,18	0,00	0,17
Hof01	15,5	0,25	0,14	0,13	0,09	0,00	0,09	0,13	0,12	0,09	0,00	0,09	0,12	0,11	0,08	0,00	0,08
Hof01>	15,5	0,19	0,25	0,23	0,17	0,00	0,16	0,24	0,22	0,16	0,00	0,16	0,22	0,20	0,15	0,00	0,14
Hof02	10	0,16	0,22	0,20	0,14	0,00	0,14	0,21	0,19	0,14	0,00	0,14	0,19	0,18	0,17	0,00	0,14
Hof02>	15,5	0,19	0,25	0,23	0,17	0,00	0,16	0,24	0,20	0,16	0,00	0,15	0,22	0,20	0,15	0,00	0,14
Hof03	10	0,16	0,22	0,20	0,14	0,00	0,14	0,21	0,19	0,14	0,00	0,14	0,19	0,18	0,10	0,00	0,12
Hof03>	10	0,12	0,33	0,30	0,21	0,00	0,21	0,31	0,28	0,20	0,00	0,20	0,28	0,26	0,10	0,00	0,16
Hof04	10	0,24	0,26	0,24	0,17	0,00	0,17	0,25	0,23	0,16	0,00	0,16	0,23	0,21	0,15	0,00	0,15
Hof05	15,5	0,37	0,19	0,18	0,13	0,00	0,13	0,18	0,17	0,12	0,00	0,12	0,17	0,15	0,11	0,00	0,11
average			0,20	0,19	0,13	0,00	0,13	0,20	0,18	0,13	0,00	0,12	0,08	0,17	0,12	0,00	0,12

Fig. 322 $\Delta C_p(z)$ for 4 flow along directions in 23 allotment types (> second measurement perpendicular)

Hof01, Hof02 and Hof03 have two main directions of front-back façades. So, ΔC_p had to be measured two times. Hoek01, Hoek04, Hof04 and Hof05 have two directions with the same characteristics perpendicular. So, the same measurement can be used the reverse (90° is 0° , 60° is 30° and so on) for the perpendicular part. Averaging the impact of both directions proportional to the number of dwellings you get numbers for corner and courtyard allotments comparable with point and line allotments.

Then we have to take other windstatistics than Northerly into account. The quarter we calculated is only very exceptionally equal to a quarter of all ventilation losses as well. This is for instance the case if that quarter (0° to 90° from y-axis) coincides with wind directions West to North. For every other North indicating arrow the calculated quarter will contribute more or less than 25% of the ventilation loss, dependent from the wind statistics exposed. This contribution is calculated for 12 North indicating arrows and completed into a 100% virtual total loss. The supposition that a dwelling surrounded by repeating allotments is equally sheltered into the other quarters is better justified than in previous paragraphs.

2.6.2 Impact of trees

Fig. 323 shows the result of this calculation on the average of Fig. 322 itemized for airtight high rise allotments and low rise ones supposed to be non airtight.

main direction	without green					with green 6m height					with green 10m height				
	0	30	60	90	virt.	0	30	60	90	virt.	0	30	60	90	virt.
average															
low rise	162	249	599	507	5162	161	247	594	506	5130	158	244	585	505	5075
high rise	90	136	343	414	3343	90	136	343	414	3343	90	136	343	414	3347

Fig. 323 Ventilation loss as a consequence of standard Northerly wind.

The impact of 6m high (young) trees is negligible. However, when for instance after 10 years trees reach a height of 10m there is some impact. However, locally the impact may be substantial (page 147).

2.6.3 Comparing repeated allotments 100x100m

Fig. 324 and Fig. 325 show some allotment types in sequence of virtual ventilation losses.

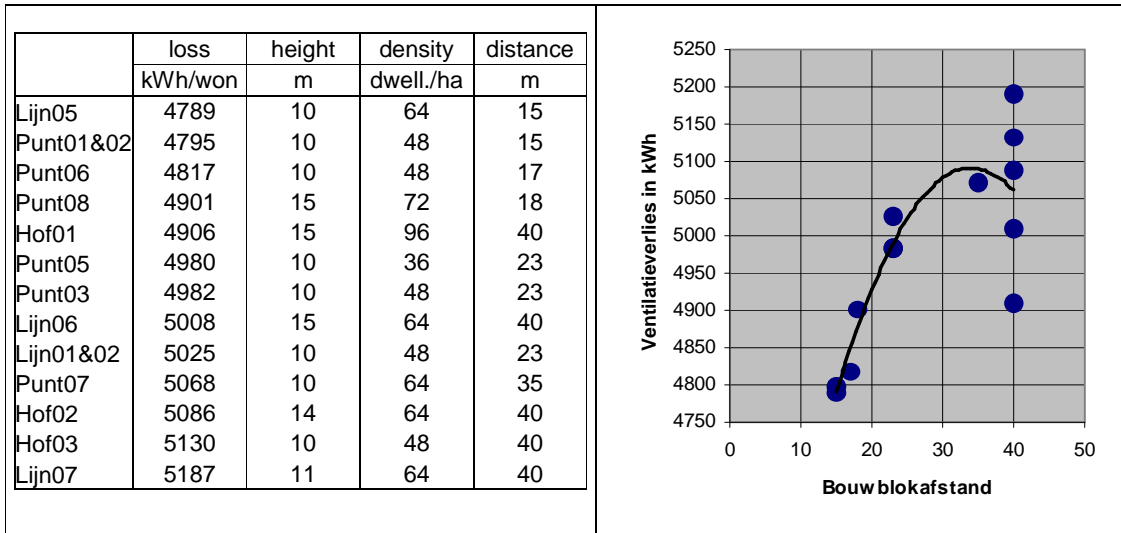


Fig. 324 Allotment types in sequence of loss

Fig. 325 Relation loss and block distance in m

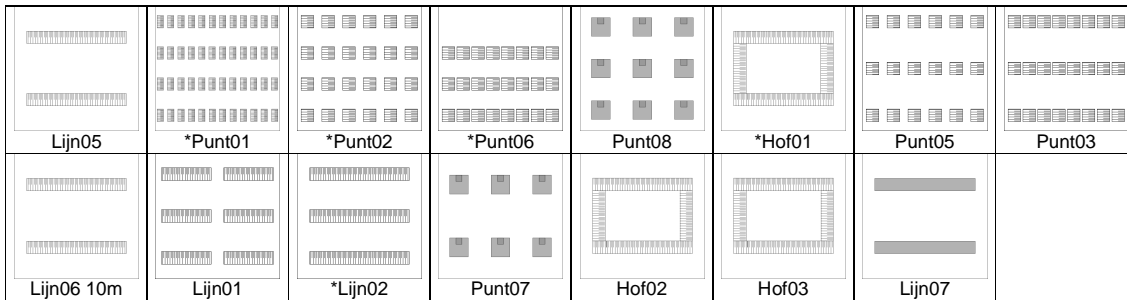


Fig. 326 Allotment types in sequence of highest to lowest loss

Remarcably there is nearly no relation with dwelling density. Lijn05 and Lijn07 of equal dwelling density (64 dwellings in the hectare concerned) and nearly the same height (10 and 11m respectively) have lowest and highest loss. However, frontal density F/O (vertical surface F per horizontal surface O) is determining (see Fig. 322) reasonably related with distance between building blocks (drawn as polynome regression in Fig. 325), but diverging at higher distances.

Fig. 327 and Fig. 328 show the results for point and line allotments on any orientation.

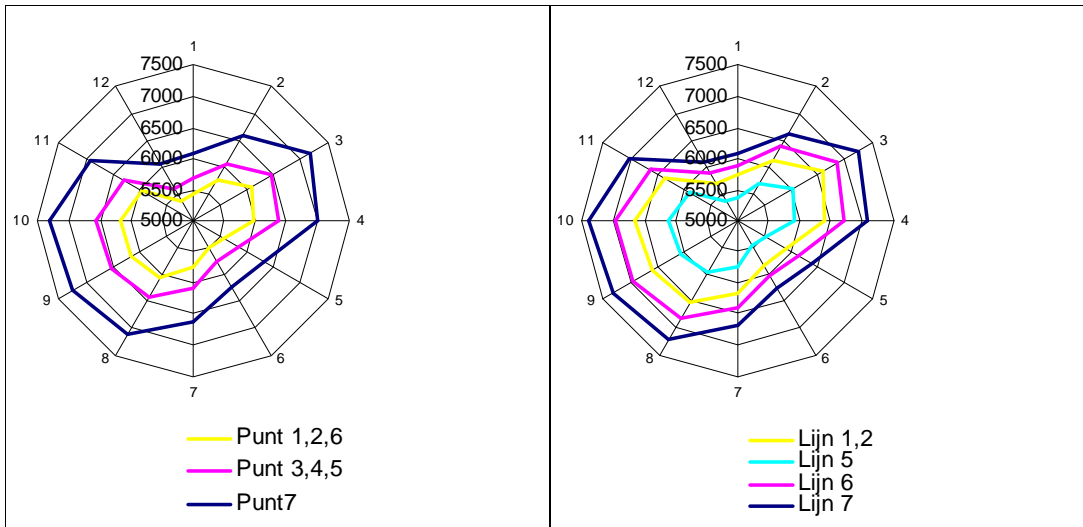


Fig. 327 Ventilation loss of point allotments

Fig. 328 Ventilation loss of line allotments

Biggest loss is reached when you orientate façades of point and line allotments 7 due West. Smallest loss is reached by line allotments 5 or point allotments 1,2 and 6 orientated on North North West (330°). The virtual difference is more than 1000kWh/dwelling.

Fig. 329 shows courtyard allotments. Orientation sensitivity levels out most in hof04 and hof05 because perpendicular blocks have equal length. Higher blocks like hof01 and hof05 (15.5m high) lose less than lower ones like hof03 and hof04 (10m).

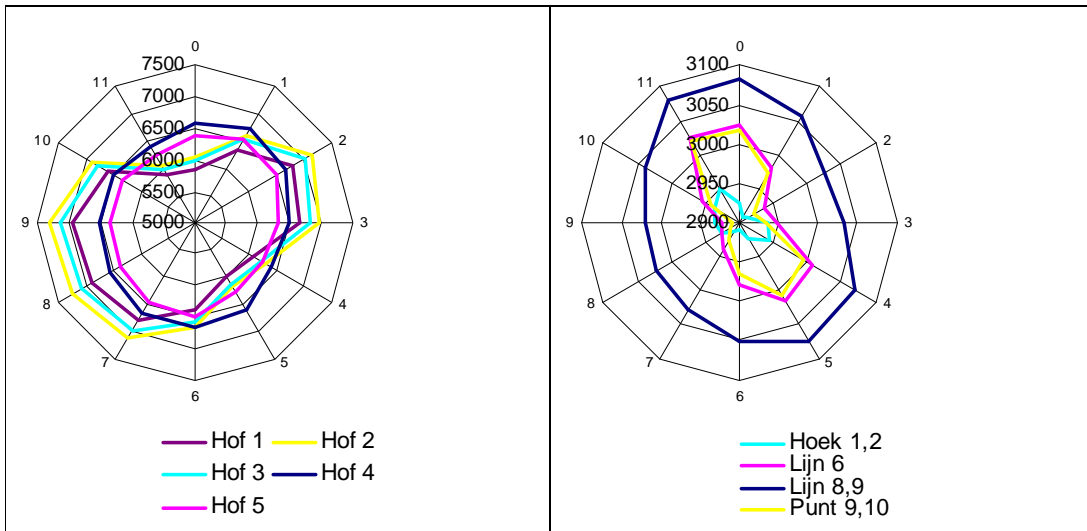


Fig. 329 Ventilation loss of courtyard allotments Fig. 330 Ventilation loss of high rise allotments

Fig. 330 shows losses of airtight high rise allotments on a much smaller scale. Total variation is less than 100kWh. Inhabitant's behaviour causes maxima where low rise non airtight allotments showed minima.

2.6.4 Wind behaviour around high objects

Wind behaviour on smallest scale is described more in detail by Voorden (1990). From that publication we derive some conclusions only. The accidental physical context and size or form of the objects cause unpredictable turbulences. Without windtunnel experiments calculations do not produce much general conclusions. However, scale models of free standing sharp edged buildings higher than 15m above the environment in a frontal flow of wind in the wind tunnel show some regularity in causing whirls windward and leeward recognisable on real scale (Fig. 331).

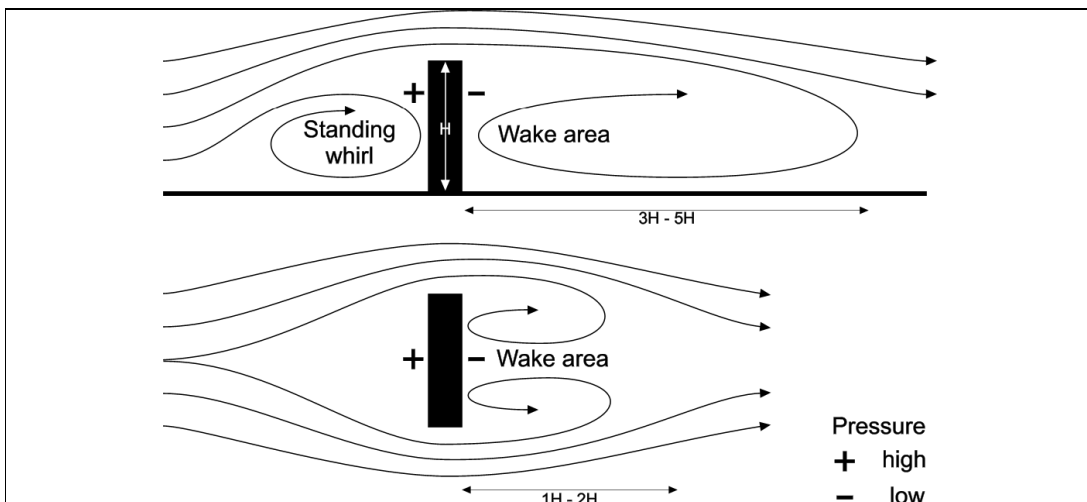


Fig. 331 Whirls around a free standing building

Windward and leeward a standing whirl arises causing unexpected wind directions on ground level. Walking or cycling along windward of the building, but especially through the wake area (zog-gebied) leeward you can experience sudden and diametral changes in wind direction. Protecting yourself with an umbrella against the wind from your left side you suddenly get wind from the right side. Fig. 331

(below) shows the same impact horizontally. The density of lines indicates wind velocity. At ground level near the edges of the building (no entrances there!) and 1H to 2H leeward, that velocity could be as high as at the top of the building. The whirls leeward are caused by low pressure on that side; the wind 'comes back' to fill the gap caused by high velocities at the edge pulling calm air with them. Openings in the building at ground level may avoid whirls there, but yield new wind velocities at ground level like Fig. 331 (below) now not considered as a plan but as a cross section.

Permeable walls like applied at the entrance of the Faculty of Architecture in Delft or dense shrubs avoid pressure differences causing whirls. They can slow down wind velocity at ground level and protect windy areas, supposed they can resist high wind velocities themselves. Networks of small wind turbines utilise local wind velocity, but they still have to be designed.

2.7 Sound and noise

2.7.1 Music

Comment [T.M.7]: Pagina: 164 kan uitbreider

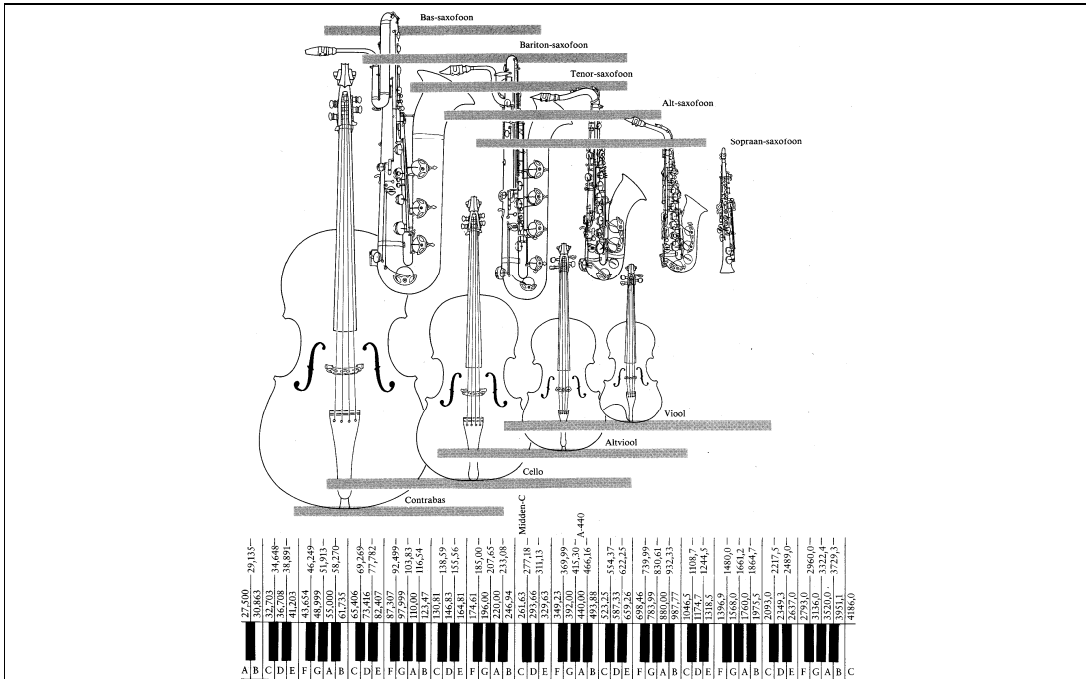
Movement of air is measured as wind when it is moving into one direction longer than 5 seconds (2.2.1). When it is flowing back in the next 5 seconds it is not even counted in wind statistics. But if the wind is blowing at average into one direction more than an hour we count it as wind and we calculate the 'hour average wind velocity' we used in chapters above. Wind is caused by slowly increasing temperature differences on the Earth's surface causing differences in air pressure. Sometimes these differences are leveled out by wind in an hour, sometimes in weeks and seldom the air is flowing back into the area it came from. If the air transported in a minute would flow back in the next minute and the reverse like water on a beach we would call it vibration. It would have a vibration time T of 60sec with a frequency f of $1/60 = 0.017$ vibrations per second or 0.017Hz (hertz).

Vibrations in the air from 16 vibrations per second (vibration time 0.063 sec) to 20 000 are accepted by our eardrums as sound. Vibrations slower than 16Hz are called infrasonic, faster than 20 000 ultrasonic. You can not hear infrasonic vibrations in the air until 16Hz, but you sometimes can feel them in your lungs Minnaert (1975). The frequencies used in music are nearly completely covered by the 88 keys of piano. It counts more than 7 octaves (Fig. 332) starting with 27.5Hz (the most left key A_1) and ending with 4186Hz (the most right key c_5 , part of the 8th octave, not fully covered).

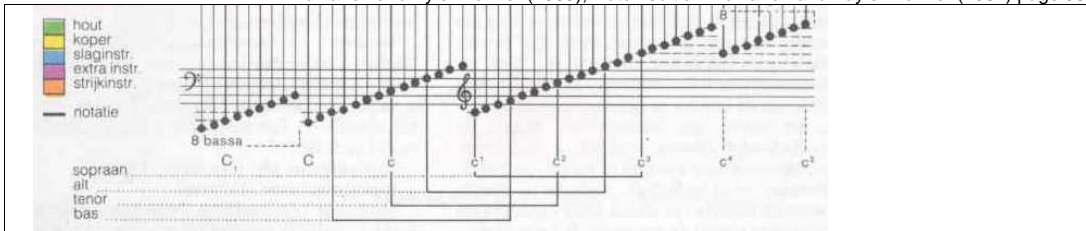
code	A_1	A	a	a_1	a_2	a_3	a_4	a_5	
frequency f	27.5	55	110	220	440	880	1760	3520	Hz
wave length λ	12.364	6.182	3.091	1.545	0.773	0.386	0.193	0.097	metres
$f \times \lambda$	340	340	340	340	340	340	340	340	m/sec

Fig. 332 Starting notes of octaves on the piano

Any next octave doubles the frequency. An octave is subdivided in 12 notes (named a, ais or bes, b, c, cis or des, d, dis or es, e, f, fis or ges, g, gis). Because $2^{1/12} = 1.0594630944$, the frequency of any next key is a factor 1.0594630944 higher than the previous one. So you can calculate the frequency of any note ($n=0\dots 87$) by $f(n)=27.5 \times 1.0594630944^n$ (Fig. 333).



McMahon and Tyler Bonner (1983), Dutch edition McMahon and Taylor Bonner (1987) page 98



Michels (1993) page 24

Fig. 333 The span of music

The travel speed of sound c in air in normal conditions 340m/sec (in steel 5064m/sec). And speed is the number of vibrations per second f times their length λ : $c=f \times \lambda$ (Fig. 332). So, the wave length λ of audible sound in air ($\lambda = c / f$) varies between $340/20\ 000 = 21.25m$ and $340/16 = 0.017m$.

Take a drawing tube of $L = 0.65m$ closed at one side (width does not matter), drum on it and you hear primarily a sound of 130Hz, which is musical note c with wave length $4 \times 0.65 = 2.60m$. But it is mixed with a specific range of overtones (Fig. 334).

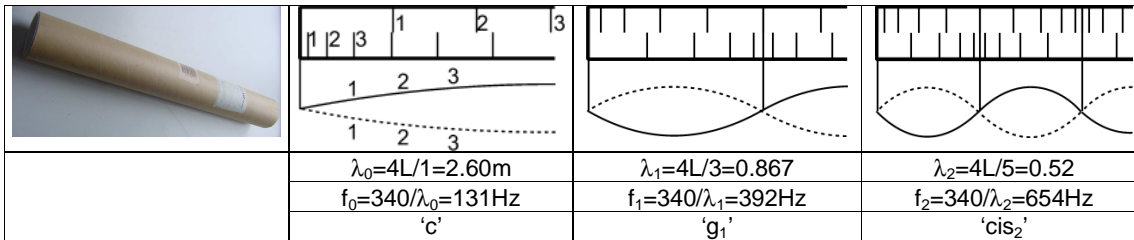


Fig. 334 Tones produced by a tube of 0.65m closed at one side.

The lines drawn in the tube represent the position of particles in extreme phases as if there were only some of them. The distance between the extreme phases (1-1, 2-2, 3-3 ...) are different, represented in the sinuses below. The closed left side of the tube forces a 'node' (line elongated into the sinus) where particles stand still as centres of condensing and thinning, the open side an 'antinode', where

they move most, enjoying the freedom of the end of the tube. So, possible wavelengths are restricted to $\lambda = 4/1, 4/3, 4/5 \dots \times L$ and frequencies to a proportion of 1:3:5.... In tubes open (antinodes) or closed (nodes) at both sides they are restricted to $\lambda = 2/1, 2/2, 2/3 \dots \times L$, supposed you do not force local antinodes by openings (like a flute does). The frequencies appear in a proportion of 1:2:3..., just like strings fixed at two sides do. A voice with less than 9 overtones sounds dim, a voice with more than 14 overtones sounds shrill.

The primary frequency of a string f_s depends on length L , tension σ and density ρ (1 290g/m³) according to $f_s = L/2 \sqrt{\sigma/\rho}$. A string with given density and tension tuned by the right force will give a lowest tone with wavelength $2 \times L$. Touching the string softly (flageolet, causing a node there without losing the lowest tone) half way you will hear a tone with wavelength L (one octave higher) as well. Touching at one third you will hear a tone with wave length $2/3 \times L$ as well, a combination called fifth (kwint, 2:3). Dividing further you get fourths (kwart, 3:4), tierces (terts, 4:5) and so on.

2.7.2 Power or intensity

Air particles between nodes move very fast around their quiet position like a sinus shown in Fig. 334 causing change in air density. Concentration causes increase of temperature and heat loss. However the particles move fast enough to prevent substantial energy loss by heat exchange (keeping the process reversible, adiabatic). The maximum divergence of particles is called amplitude A . The power of a sound wave (called intensity 'I' and expressed in W/m²) depends on that amplitude, but also on frequency f , air density (normally 1.290kg/m³), and travel speed (normally 340m/sec) according to $I = \rho \times (2 \times \pi \times f \times A)^2 \times c/2$. So, in normal p and c conditions power depends on amplitude A and frequency f according to $I = 8658 \times (f \times A)^2$.

A speaking voice produces $10^{-5} W$. A globe with a radius of 28cm has a surface of $1m^2$. So, at 28cm distance that voice has a power of $10^{-5} W/m^2$. It is composed by adding $8658 \cdot (f \times A)^2$ for every frequency and its accompanying amplitude in the voice. But suppose it produces tone c only, without overtones (in reality produced by electronic device only), then frequency is 131Hz, and amplitude A should be 0.000003m. A piano produces maximally $0.2W/m^2$ and if it would be produced by tone c only the amplitude should be 0.0000367m. For an extended symphony orchestra and a loudspeaker the figures would be $5W/m^2$ ($A=0.0000183m$) and $100W/m^2$ ($A=0.00082m$). Fig. 336 shows the dependency of intensity I on these particular amplitudes and on musical frequencies from 27.5 to 4000Hz).

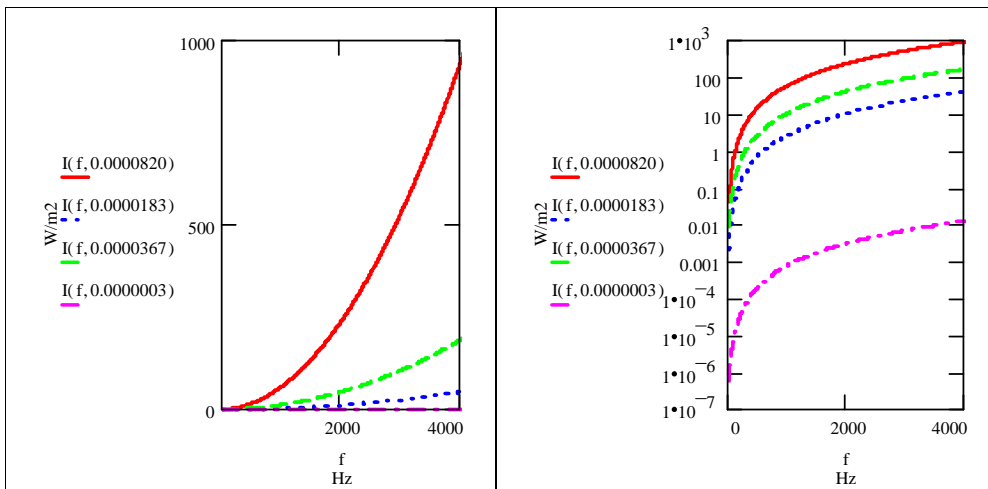


Fig. 335 Intensity (frequency, amplitude)

Fig. 336 Represented logarithmically

The logarithmical representation (Fig. 336) shows the range from soft to loud better. Dividing the intensity by a standard of $10^{-12} W/m^2$ (comparing it with that standard) we get positive logarithms from 0 to 14 only, starting with what is just audible. Multiplying it by 10 we get a useful range of decibells (dB) from 0 to 150 (Fig. 337).

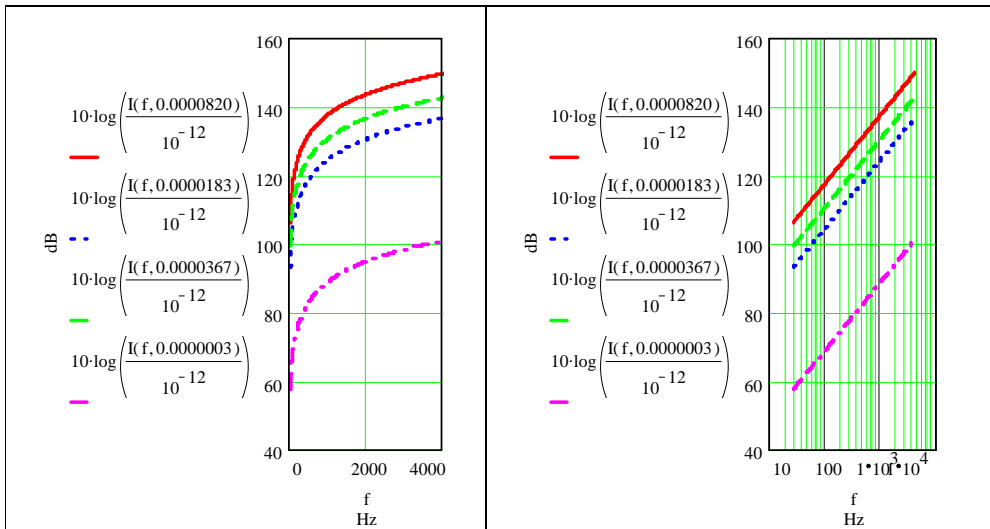
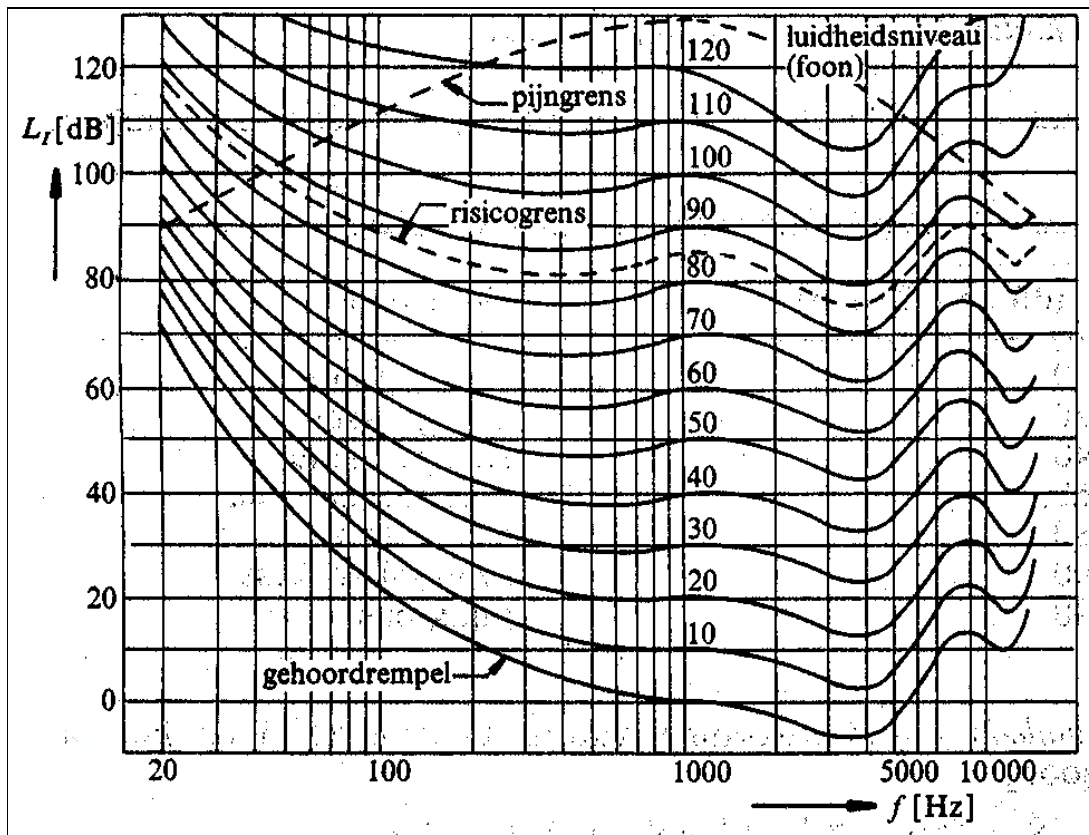


Fig. 337 Changing intensity into decibells

Fig. 338 Represented logarithmically

Changing the frequency axis in a logarithmical scale (Fig. 338) we get beautiful straight lines of growing decibells by increasing frequencies for every amplitude. Fig. 339 is the same graph with the boundary of what we think to hear.



Creemers, Atteveld et al. (1983) page 186

Fig. 339 Pain boundary (above) and impression of sound.

At 1000Hz our impression of sound could be approximated by deciBells. However, on both sides of this centre we hear less from the actual pressure of lower and higher tones on our eardrums. That can be dangerous. Lines of equal sound impression more or less parallel to the boundary below connect the same levels of sound impression (loudness) expressed in 'foons' in the same range of deciBells at 10^3 Hz. An often used rough correction is the audible deciBell dB(A) (Fig. 340).

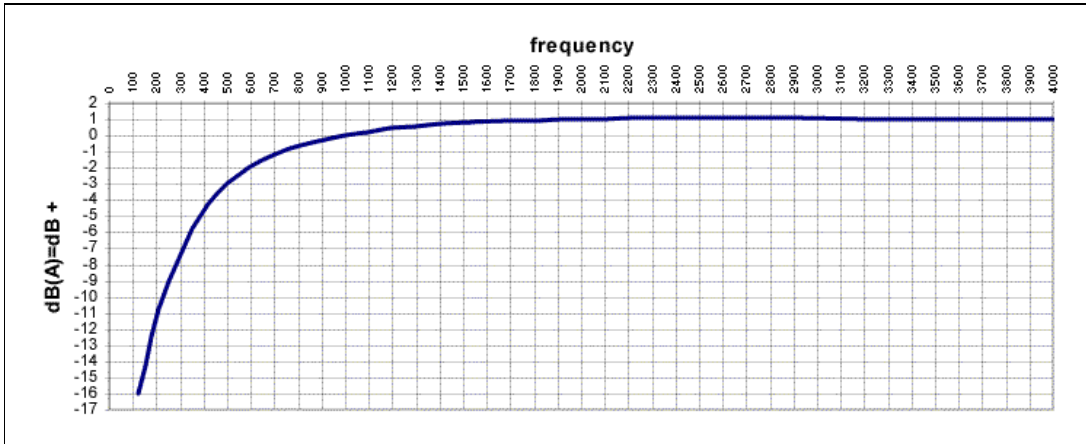


Fig. 340 Corrections on deciBells to get audible dB(A).

2.7.3 Sound and noise

The combined tones of an instrument make a sound. When we complete the sinuses into $\lambda = 4 \times 0.65\text{m}$ and add the overtones of Fig. 334 with supposed smaller amplitudes neglecting the higher overtones we get a representation of the sound of the tube (Fig. 341).

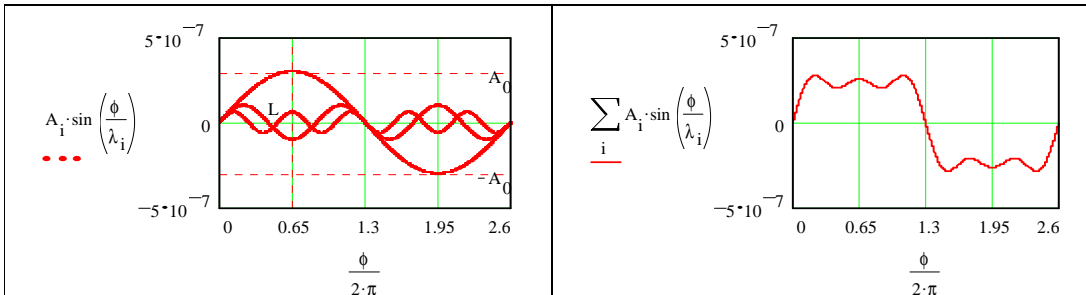


Fig. 341 Combined complete sinuses of Fig. 334

Fig. 342 Fig. 341 added

However, especially string instruments have to improve the contact with the air by surfaces vibrating with the string to get a louder sound. These constructions resonate with the own velocities, amplitudes and frequencies of their material and form adding new wave lengths producing the typical sound of the instrument. The amplitudes per frequency are called the spectrum of the instrument (Fig. 343 and Fig. 344).

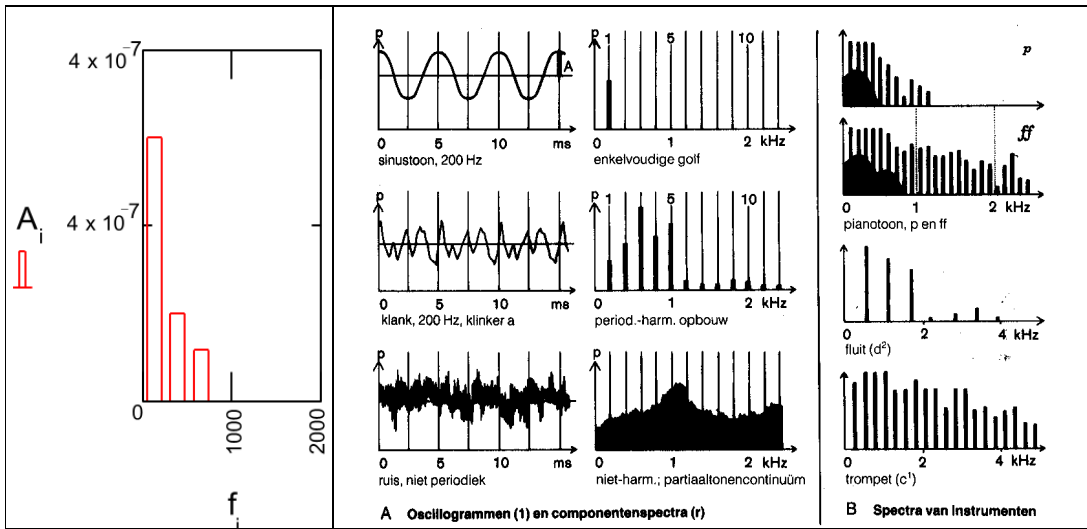


Fig. 343 Supposed amplitudes of the tube from Fig. 334

Fig. 344 Spectra of other instruments

Michels (1993) page 16

There are harmonious spectra with natural proportions of frequencies and chaotic spectra called noise. When you are able to recognise the composing sinuses by Fourier analysis or measurement you can calculate the power of a spectrum summing all intensities per amplitude by integration to predict power. But there are deciBell meters to do it afterwards.

2.7.4 Birds

Fig. 345 shows the spectrum of an electric piano with little overtones for the tone 'A' in eight octaves with seconds on the x-axis. Here we clearly see the doubling from 27.5, 55, 110, 220, ... until 3520 kHz for pure tones. The tones of the piano fluctuate around these averages.

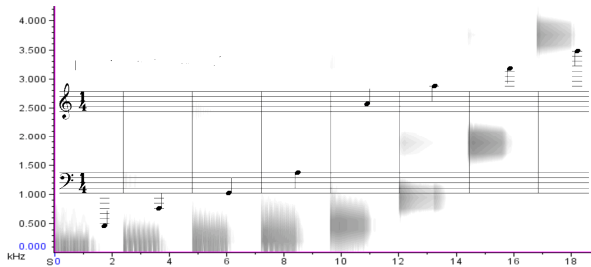


Fig. 345 Spectrum of an electric piano

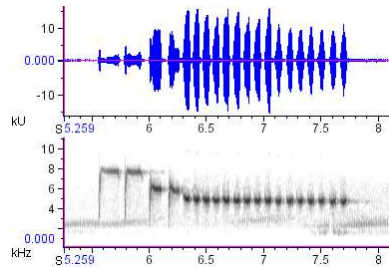


Fig. 346 Oscillogramme and spectrum of a bluetit (pimpelmees)

Fig. 346 we see the spectrum of a bluetit-song with frequencies reaching twice as high as our voice until 8 kHz. The oscillogramme above shows the amplitude or power. Enlargement would show the sinusoid waves. Their invisibly small wave-lengths determine the frequency below. Fig. 347, Fig. 348 and Fig. 349 show the oscillogrammes and spectra of three other birds often heard around your house. They show how characteristic birds' songs are. These songs are present in any city, but you don't hear them any more and few will recognise them.

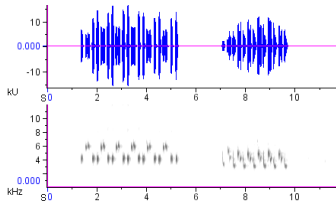


Fig. 347 Great tit (koolmees)

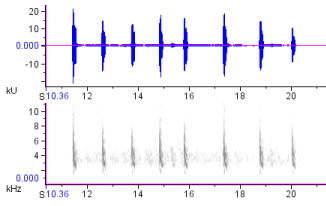


Fig. 348 House sparrow (huismus)

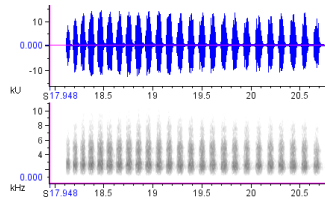


Fig. 349 Magpie (ekster)

These spectra are made with the Raven Lite programme, free downloadable from <http://www.birds.cornell.edu/brp/raven/Raven.html>.

2.7.5 Traffic noise

There are many sources of noise in town. Traffic and aviation are the most important ones.

	speed	quantity	emission
	km/h	mv/h	dB(A)
light motor vehicles	50	300	69,48
middle heavy motor vehicles	50	50	72,90
heavy motor vehicles	50	50	77,70
motorcycles	50	100	75,21
Total		500	80,81+
% truck traffic	10%		
road surface			
Road surface correction			3,63+
distance to crossing	100m		
Crossing correction			0,80+
%reflection other side of road	75%		
Reflection correction			1,13+
distance to source	10m		
Distance reduction			10,00-
Air muffling reduction			0,20-
height of observer	1,5m		
height of source	0m		
%soft ground to road axis	0%		
Ground reduction			0,00-
Meteo reduction			0,57-
Total			75,59dB(A)

Jong (2003)

Fig. 350 Calculating traffic noise

Traffic is a linear and fluctuating source. You can predict the average intensity in dB(A) from 7 o'clock during 12 hours day or night according to Volksgezondheid Volksgezondheid en Milieuhygiene (1981), SRM1, see Fig. 350. Backgrounds are discussed in Nijs (1995). Download Jong, T.M. de (2003) *TrafficNoise.xls* from <http://team.bk.tudelft.nl> publications 2003, say 'yes' to the macro's, fill in the yellow parts and try.

TRAFFIC NOISE

This calculation is valid only if:

- there are no noise protection screens or buildings;
- there are no slopes;
- the road is more or less straight;
- some other conditions,

otherwise you should use SRM2.

Fig. 351 shows some indications for traffic load you can use in designing stage.

Indication:

radius served	urban area	traffic lanes	width	mv/h
30m		1	3m	2
100m	street	2	10m	20
300m	neighbourhood street	2	20m	200
1km	district road	2	30m	1000
3km	town highway	4	40m	2000
10km	subregional highway	8	50m	10000
30km	regional highway	10	60m	16000
100km	subnational highway	16	70m	24000

Fig. 351 Indications of traffic load

National Law (see www.overheid.nl click Wet- en regelgeving, look for 'geluidhinder') demands in new plans for urban area less than 50 dB(A) within 200m from streets with 1 or 2 traffic lanes or within 350m from roads and highways with more than 2 traffic lanes causing that amount of noise. But Burgomaster and Aldermen can request the Provincial Council on the basis of a noise survey to increase the norm to 55 dB(A). In special cases named in the Law it can be increased until 70 dB(A). Comparable norms are given for other sources like industry.

To calculate noise from aeroplanes Kosten units (Ke) are used. They take into account maximum level of noise per movement, number of movements per year and time of the day.